

The complexity of blocking bivalent protein-protein interactions: development of a highly potent inhibitor of the menin-Mixed Lineage Leukemia (MLL) interaction

Dmitry Borkin, Szymon Klossowski, Jonathan Pollock, Hongzhi Miao, Brian Linhares, Katarzyna Kempinska, Zhuang Jin, Trupta Purohit, Bo Wen, Miao He, Duxin Sun, Tomasz Cierpicki, and Jolanta Grembecka

J. Med. Chem., **Just Accepted Manuscript** • DOI: 10.1021/acs.jmedchem.8b00071 • Publication Date (Web): 08 May 2018

Downloaded from <http://pubs.acs.org> on May 8, 2018

Just Accepted

“Just Accepted” manuscripts have been peer-reviewed and accepted for publication. They are posted online prior to technical editing, formatting for publication and author proofing. The American Chemical Society provides “Just Accepted” as a service to the research community to expedite the dissemination of scientific material as soon as possible after acceptance. “Just Accepted” manuscripts appear in full in PDF format accompanied by an HTML abstract. “Just Accepted” manuscripts have been fully peer reviewed, but should not be considered the official version of record. They are citable by the Digital Object Identifier (DOI®). “Just Accepted” is an optional service offered to authors. Therefore, the “Just Accepted” Web site may not include all articles that will be published in the journal. After a manuscript is technically edited and formatted, it will be removed from the “Just Accepted” Web site and published as an ASAP article. Note that technical editing may introduce minor changes to the manuscript text and/or graphics which could affect content, and all legal disclaimers and ethical guidelines that apply to the journal pertain. ACS cannot be held responsible for errors or consequences arising from the use of information contained in these “Just Accepted” manuscripts.

1
2
3 **The complexity of blocking bivalent protein-protein interactions: development of a highly**
4 **potent inhibitor of the menin-Mixed Lineage Leukemia (MLL) interaction**
5
6
7

8 Dmitry Borkin^{a,#}, Szymon Klossowski^{a,#}, Jonathan Pollock^a, Hongzhi Miao^a, Brian M. Linhares^a,
9 Katarzyna Kempinska^a, Zhuang Jin^a, Trupta Purohit^a, Bo Wen^b, Miao He^b, Duxin Sun^b, Tomasz
10 Cierpicki^a, Jolanta Grembecka^{a,*}
11
12
13
14
15

16
17
18 ^a Department of Pathology, University of Michigan, Ann Arbor, MI, 48109, USA
19

20 ^b College of Pharmacy, University of Michigan, Ann Arbor, MI, 48109, USA
21

22 [#] D.B. and S. K. contributed equally to this work
23
24
25

26
27 ^{*}Corresponding author;
28

29 Jolanta Grembecka, PhD
30

31 Associate Professor,
32

33 Department of Pathology,
34

35 University of Michigan
36

37 1150 West Medical Center Dr, MSRB I, Room 4510D
38

39 Ann Arbor, MI, 48108
40

41 e-mail: jolantag@umich.edu
42

43 Tel. 734-615-9319
44
45
46
47
48
49
50
51
52
53
54
55
56
57
58
59
60

Abstract

The protein-protein interaction between menin and Mixed Lineage Leukemia 1 (MLL1) plays an important role in development of acute leukemia with translocations of the *MLL1* gene and in solid tumors. Here, we report the development of a new generation of menin-MLL1 inhibitors identified by structure-based optimization of the thienopyrimidine class of compounds. This work resulted in compound **28** (**MI-1481**), which showed very potent inhibition of the menin-MLL1 interaction ($IC_{50} = 3.6$ nM), representing the most potent reversible menin-MLL1 inhibitor reported to date. The crystal structure of the menin-**28** complex revealed a hydrogen bond with Glu366 and hydrophobic interactions, which contributed to strong inhibitory activity of **28**. Compound **28** also demonstrates pronounced activity in MLL leukemia cells and *in vivo* in MLL leukemia models. Thus, **28** is a valuable menin-MLL1 inhibitor that can be used for potential therapeutic applications and in further studies regarding the role of menin in cancer.

Introduction

Menin is a scaffold protein that is involved in a network of protein-protein interactions, among which the interaction with the Mixed Lineage Leukemia 1 (MLL1; hereafter referred as MLL) protein or MLL fusion proteins have been recognized as highly relevant to human diseases, specifically to cancer.¹ The *MLL1* gene is translocated in 5-10% of acute leukemia cases, and this translocation leads to the expression of MLL fusion proteins, which are critical drivers of leukemogenesis.²⁻³ The MLL leukemia patients have an approximately 35% five-year survival rate,⁴⁻⁵ which reflects poor response to currently available treatments and supports the need for the development of new therapies. The interaction of menin with MLL fusion proteins plays a key role in leukemogenesis, which was demonstrated before using genetic approaches.^{2, 6-7} The importance of this interaction in MLL leukemia has been further validated by small molecule inhibitors of the menin-MLL interaction that we have reported in earlier studies.⁸⁻¹² Furthermore, the interaction of menin with the wild type MLL plays an important role in solid tumors, including castration resistant prostate cancer,¹³ Ewing sarcoma,¹⁴ hepatocellular carcinoma (HCC)¹⁵⁻¹⁶ and pediatric gliomas.¹⁷ Therefore, the development of small molecule inhibitors of the menin-MLL interaction with optimized drug-like properties may lead to new therapeutics for acute leukemia and a subset of solid tumors.

The development of potent inhibitors with favorable drug-like properties that target protein-protein interactions (PPI) is still a challenge.¹⁸⁻¹⁹ The specific architecture of protein-protein interfaces (e.g. the lack of well-defined pockets and large contact areas) frequently implies the need for increasing the molecular weight of PPI inhibitors, which makes it difficult to achieve strong potency and favorable drug-like properties.²⁰ Nevertheless, successful examples of PPI inhibitors exist,²¹⁻²⁴ including compounds advanced to clinical trials (e.g. Bcl-2 family inhibitors, p53 activators²⁵⁻²⁶), thus supporting efforts in this direction. Furthermore, the recent FDA

1
2
3 approval of the BCL-2 inhibitor Venetoclax demonstrates that PPI inhibitors can be valuable
4 therapeutics, despite challenges it obtaining favorable drug-like properties for such compounds
5 as a result of inherently higher than average molecular weight ($M_w > 800$ Da for Venetoclax).
6
7

8
9
10 The protein-protein interaction between menin and MLL or MLL fusion proteins involves
11 the N-terminal fragment of MLL (MLL_{4-43})^{2, 6}, which binds to menin with a strong binding
12 affinity ($K_d = 6.8$ nM) by utilizing the bivalent binding mode, with MBM1 (menin-binding motif
13 1, MLL_{4-15}) and MBM2 (menin-binding motif 2, MLL_{23-43}) motifs involved in the interactions
14 with menin.²⁷ Structural studies have revealed that MLL binds to a large central cavity on
15 menin,^{9, 28} thus supporting the existence of pockets to bind small molecules. Indeed, our previous
16 studies have validated that the menin-MLL interaction can be effectively blocked with small
17 molecules that bind to the MLL binding site on menin.⁸⁻¹² However, due to the extended menin-
18 MLL interface resulting from the bivalent binding mode of MLL to menin, optimization of the
19 potency and drug-like properties of menin-MLL inhibitors remains challenging.¹²
20
21
22
23
24
25
26
27
28
29
30
31
32

33 Our previous efforts resulted in the development of the thienopyrimidine class of menin-
34 MLL inhibitors, with **MI-463**, **MI-503** and **MI-538** demonstrating the most potent inhibitory
35 activity (**Figure 1a**).^{10, 12} These compounds selectively block proliferation of human MLL
36 leukemia cells ($GI_{50} = 200-500$ nM), demonstrate specific mechanism of action and delay
37 leukemia progression in mice models of MLL leukemia.^{10, 12} **MI-503** also demonstrated activity
38 in prostate cancer,¹³ Ewing sarcoma¹⁴ and hepatocellular carcinoma¹⁶ models. However, menin-
39 MLL inhibitors with improved therapeutic potential over **MI-503**, namely with increased
40 potency (e.g. $IC_{50} < 10$ nM to make them comparable or more potent than MLL_{4-43} , $GI_{50} < 50$
41 nM and >100 -fold selectivity to MLL leukemia cells, strong reduction in leukemia burden and
42 $>50\%$ decrease in target gene expression *in vivo*) are still required. In this study we report
43
44
45
46
47
48
49
50
51
52
53
54
55
56
57
58
59
60

1
2
3 structure-based optimization of the **MI-463** and **MI-503** menin-MLL inhibitors by exploring a
4 collection of saturated six-membered rings introduced at the indole nitrogen of these compounds
5
6 to further improve their activity and drug-like properties. These efforts resulted in the
7
8 identification of compound **28** (**MI-1481**), which demonstrated low nanomolar activity ($IC_{50} =$
9
10 3.6 nM) for the inhibition of the interaction between menin and the bivalent MLL₄₋₄₃
11
12 encompassing the entire menin binding motif on MLL. Thus, **28** demonstrates >10-fold
13
14 improved inhibitory activity over **MI-503**, representing the most potent reversible small
15
16 molecule menin-MLL inhibitor reported to date. Compound **28** also demonstrated substantially
17
18 increased activity in MLL leukemia cells (~10-fold) over the previous generation of reversible
19
20 menin-MLL inhibitors,^{10, 12} high selectivity towards MLL leukemia cells and pronounced *in vivo*
21
22 activity in a mice model of MLL leukemia. We also report the co-crystal structure of the menin-
23
24 **28** complex, which revealed that both polar and hydrophobic interactions likely contribute to the
25
26 strong inhibitory activity of this compound. This compound could serve as a valuable chemical
27
28 probe to further study the role of menin in pathological and physiological states and could lead to
29
30 the development of a new therapeutic agent for tumors that rely on menin-MLL interaction.
31
32
33
34
35
36
37
38
39

40 **Results and Discussion**

41 **Biochemical assay to assess potent menin-MLL inhibitors**

42
43 We have recently reported the thienopyrimidine class of menin-MLL interaction, with the most
44
45 potent **MI-463** (compound **1**) and **MI-503** (compound **2**), **Figure 1a**, **Table 1**.^{10, 12} These
46
47 compounds bind to menin with $K_d \sim 10$ nM and block the interaction of menin with a short
48
49 MLL-derived peptide MBM1 (MLL₄₋₁₅) with nanomolar inhibitory activities ($IC_{50} \sim 15$ nM for
50
51 both compounds) as measured in the fluorescence polarization (FP) assay, **Figure 1a**. However,
52
53 in the FP competition assay the low end of inhibitor K_i values that can be accurately measured is
54
55
56
57
58
59
60

1
2
3 the K_d value of the fluorescent ligand, and for inhibitors more potent than the fluorescent probe
4
5 the IC_{50} values are independent of inhibitor potency but linearly proportional to the K_d value of
6
7 the fluorescence ligand.²⁹ Based on the modest binding affinity of the fluorescein labeled (FLSN)
8
9 MBM1 to menin ($K_d = 49$ nM)²⁷ we concluded that menin-MLL inhibitors with low nanomolar
10
11 binding affinity or better would reach the detection limit of the competition FP assay that uses
12
13 FLSN_MBM1. To avoid this issue, we utilized the bivalent fragment of MLL (MLL₄₋₄₃) in the
14
15 competition FP assay for testing of the new generation of menin-MLL inhibitors. The MLL₄₋₄₃
16
17 includes the entire menin binding motif (MBM1 and MBM2)^{6, 27} and binds to menin with $K_d =$
18
19 6.8 nM as determined by the Isothermal Titration Calorimetry (ITC). First, we determined the
20
21 binding affinity of the fluorescein labeled MLL₄₋₄₃ peptide (FLSN-MLL₄₋₄₃) to menin in this new
22
23 FP assay, resulting in $K_d = 1.0$ nM **Supplementary Figure 1**, which remains in a good
24
25 agreement with the results from the ITC experiment.²⁷ We then applied the FP competition assay
26
27 with FLSN-MLL₄₋₄₃ to test the inhibitory activity of **MI-463** and **MI-503** menin-ML inhibitors,
28
29 resulting in IC_{50} values of 32 and 33 nM, respectively, **Figure 1a, Table 1**. Because MLL₄₋₄₃
30
31 encompasses the entire menin binding motif, these data support that the thienopyrimidine
32
33 compounds (e.g. **MI-463** and **MI-503**) can effectively displace the bivalent MLL fragment from
34
35 menin, which is an important feature in the context of functional studies. Overall, based on these
36
37 results we concluded that the FP assay utilizing the bi-valent MLL₄₋₄₃ peptide represents an
38
39 appropriate approach to provide accurate activity measurements for low nanomolar inhibitors of
40
41 the menin-MLL interactions. Thus, we used this assay to assess the *in vitro* activity of all
42
43 compounds reported in this study.
44
45
46
47
48
49
50
51
52
53

54 **Development of menin-MLL inhibitors with saturated rings substituting indole nitrogen**

55
56
57

1
2
3 In our previous studies, we developed **MI-463** and its analogues with different substitutions at
4 the indole ring, including aliphatic and aromatic substituents on indole nitrogen (e.g. **MI-503**),
5 **Figure 1a**. However, these modifications did not result in increased inhibitory activity as
6 compared to **MI-463**.¹² To further optimize these compounds we performed detailed analysis of
7 the co-crystal structure of menin in complex with **MI-503**, which revealed three hydrogen bonds
8 (with Tyr276, Trp341 and Glu366) and hydrophobic interactions with menin,¹⁰ **Figure 1b**.
9 Furthermore, we found that the methyl-pyrazole ring substituting indole nitrogen in **MI-503** is
10 partly solvent exposed, with two negatively charged residues on menin, Glu363 and Glu366,
11 approaching this ring, **Figure 1b**. Based on this analysis we designed various saturated rings
12 harboring positively charged and/or uncharged polar groups to be introduced at the indole
13 nitrogen of **MI-463** to form electrostatic interactions or hydrogen bonds with this area of the
14 binding site on menin.
15
16
17
18
19
20
21
22
23
24
25
26
27
28
29

30
31 First, we explored several saturated rings with short aliphatic linkers substituting indole
32 nitrogen of **MI-463**, **Table 1**. Introduction of the piperazine or piperidine rings, which resulted in
33 compounds **3** and **4**, **Table 1**, led to a ~2-fold improved inhibitory activity over **MI-463** (IC_{50} =
34 15 and 14 nM for **3** and **4**, respectively). On the other hand, incorporation of the morpholine
35 (compound **5**) or morpholinone (compound **6**) rings connected to indole through an ethyl linker
36 resulted in less pronounced activity improvement (<1.5-fold) over **MI-463**, **Table 1**.
37 Interestingly, the introduction of the methyl-morpholinone substituent at indole nitrogen
38 (compound **7**, **MI-568**) resulted in an over 4-fold improvement in the IC_{50} value (IC_{50} = 7.5 nM
39 for the racemic mixture of **7**) as compared to **MI-463**, **Table 1**. Thus, although **7** represents the
40 racemic mixture of two enantiomers, this compound demonstrates low nanomolar inhibition of
41
42
43
44
45
46
47
48
49
50
51
52
53
54
55
56
57
58
59
60

1
2
3 the menin-MLL interaction, outperforming other compounds with various saturated rings
4 introduced to the scaffold, **Table 1**.

5
6
7
8 We then assessed the cellular activity in MLL leukemia cells and the microsomal stability
9 of compounds **3-7**, **Table 1**. Notably, compound **7** demonstrated the most pronounced effect on
10 proliferation of the MLL-AF9 transformed leukemia cells ($GI_{50} = 50$ nM), representing ~5-fold
11 stronger cellular activity than **MI-463**, **Table 1**. The cellular activities of compounds **3-6** are less
12 pronounced and range from 0.15-0.81 μ M, **Table 1**. Interestingly, despite improved inhibitory
13 activity, compounds **3** and **4** showed weaker cell growth inhibition as compared to **MI-463**,
14 which may have resulted from the positive charge in the piperazine or piperidine rings of these
15 compounds, possibly affecting their cellular permeability. In addition, compounds **3**, **4** and **7**
16 showed the best microsomal stability measured in mouse liver microsomes ($T_{1/2} > 60$ min),
17 representing substantial improvement over **MI-463** or **MI-503**, **Table 1**. Furthermore, compound
18 **7** has also the lowest clogP value (**Table 1**), thus supporting favorable polarity and solubility.
19 Overall, these results support that the analogues of **MI-463** with saturated rings introduced at
20 indole nitrogen represent valuable candidates for further optimization.
21
22
23
24
25
26
27
28
29
30
31
32
33
34
35
36
37
38
39

40 **Optimization of analogues with piperazine ring**

41
42 Since compound **3** showed 2-fold improvement in inhibitory activity and substantially increased
43 metabolic stability over **MI-463** (**Table 1**), we pursued further optimization of **3** by introducing
44 substituents to the piperazine ring. First, we introduced aliphatic groups, such as methyl
45 (compound **8**) and *n*-propyl (compound **9**), but they did not improve substantially the *in vitro*
46 inhibitory activity or cell growth inhibition in MLL-AF9 cells over **3**, **Table 2**. Analysis of the
47 crystal structure of the menin-**MI-503** complex revealed the presence of Arg330,¹⁰ which could
48
49
50
51
52
53
54
55
56
57
58
59
60

1
2
3 potentially be involved in hydrogen bond/salt bridge with ligands that harbor the appropriate
4 substituent at the indole nitrogen of **MI-463**. Therefore, we introduced the formamide group to
5
6 the piperazine ring (compound **10**), but this modification did not improve inhibitory activity
7
8 (IC₅₀ = 13 nM for **10**), although activity in the MLL-AF9 transformed cells demonstrated a 2-
9
10 fold improvement for **10** over **3**, **Table 2**. This was likely due to the neutralization of the positive
11
12 charge in **3**, which could have positively affected the cellular permeability. Further substitution
13
14 of the amide with methyl (compound **11**) did not significantly change the inhibitory activity,
15
16 while ethyl analog (compound **12**) showed an over 6-fold reduction in inhibitory activity (IC₅₀ =
17
18 83 nM) as compared to **10**. Interestingly, the analogue with the monofluoromethyl group
19
20 (compound **13**, **MI-853**) demonstrated slightly improved inhibitory activity (IC₅₀ = 10 nM) over
21
22 **10**, while the di- and trifluoromethyl analogues (**14** and **15**) were 2-5-fold less potent than **10**,
23
24 **Table 2**. Improved *in vitro* activity of **13** resulted in more potent cell growth inhibition of the
25
26 MLL-AF9 transformed cells observed for this compound (GI₅₀ = 75 nM), **Table 2**. Furthermore,
27
28 introduction of a larger hydrophobic group substituting amide in **10**, which resulted in
29
30 compounds **16** and **17**, led to a 3-4-fold reduced inhibitory activity, **Table 2**. Finally, we
31
32 introduced the 2-propanamide group (compound **18**), but did not observe increased inhibitory
33
34 activity for the racemic mixture of this compound over **10**, **Table 2**.
35
36
37
38
39
40
41

42 To further explore substitutions at the piperazine ring of **3**, we substituted this ring with
43
44 sulfonyl or sulfonamide groups (compounds **19-23**), **Table 2**. Among these compounds the
45
46 analogue with the methyl sulfonamide (compound **19**), demonstrated the most pronounced
47
48 inhibitory activity for blocking the menin-MLL interaction (IC₅₀ = 13 nM), **Table 2**. The
49
50 structure-activity relationship for the sulfonyl analogues (compounds **19-23**) is similar to the
51
52 corresponding amide derivatives, **Table 2**, with reduced inhibitory activity upon increasing the
53
54
55
56
57
58
59
60

1
2
3 size of the aliphatic substituent (e.g. compounds **20** and **21**, **Table 2**). The sulfamide derivatives
4
5 **22** and **23** showed about 2-fold reduction in inhibitory activity as compared to the methylsulfone
6
7 analogue **19**, **Table 2**.
8
9

10 Despite comparable or weaker inhibitory activity in *in vitro* biochemical assay, the
11 majority of compounds with amides, sulfones or sulfonamides substituting the piperazine ring in
12
13 **3** demonstrated stronger cell growth inhibition of the MLL-AF9 transformed cells (GI_{50} values
14
15 below 200 nM) as compared to compound **3**, **Table 2**. This may have resulted from the reduced
16
17 basicity of these compounds over **3**, which could have affected their cellular permeability.
18
19 Importantly, the piperazine analogues demonstrated good correlation of *in vitro* inhibitory
20
21 activity with cell growth inhibition, with compound **13** showing the strongest inhibitory activity
22
23 ($IC_{50} = 10$ nM) for blocking the menin-MLL interaction and inhibition of cell proliferation in
24
25 MLL-AF9 leukemia cells ($GI_{50} = 75$ nM), **Table 2**. On the other hand, the microsomal stability
26
27 of the amide and sulfonamide analogues is reduced as compared to compound **3** (**Table 2**),
28
29 although compounds **19** and **22** still retain relatively good microsomal stability ($T_{1/2} > 25$ min).
30
31
32
33
34
35
36
37

38 **Development of analogues with substituted piperidine ring**

39
40 Because unsubstituted piperazine (**3**) and piperidine (**4**) derivatives have similar inhibitory
41
42 activity in blocking the menin-MLL interaction, we also explored several analogues derived
43
44 from **4**, **Table 3**. In contrast to the corresponding piperazine analogues, the introduction of the
45
46 amide group (compound **24**) and its further substitution with methyl (compound **25**) resulted in a
47
48 5-10 fold reduction in inhibitory activity as compared to **4**, **Table 3**. Similarly, the incorporation
49
50 of the sulfonamide (compound **26**) or sulfamide (compound **27**) groups to this scaffold resulted
51
52 in >2-fold reduced inhibitory activity over **4**, **Table 3**. Based on these results we concluded that
53
54
55
56
57

1
2
3 the reduced basicity of the piperidine series (**Table 3**) makes these compound less potent menin-
4 MLL inhibitors than the corresponding piperazine derivatives (**Table 2**) possibly due to the
5 absence of long-range electrostatic interactions with Glu363 and/or Glu366 side chains, **Figure**
6
7
8 **1b**. Interestingly, despite weaker *in vitro* inhibitory activity, all piperidine analogues
9 demonstrated comparable or increased activity in MLL leukemia cells over **4** (e.g. compound **26**
10 has over 3-fold improved GI₅₀ as compared to **4**, **Table 3**). Furthermore, compounds **24-27**
11 demonstrate good microsomal stability, with the sulfonyl (**26**) or sulfonamide (**27**) analogues
12 exhibiting the longest half-life in mouse liver microsomes ($T_{1/2} > 60$ min).
13
14
15
16
17
18
19
20
21
22
23

24 **Structural studies reveal the binding mode of piperazine derivatives to menin**

25
26 To understand the molecular basis of the interactions of the piperazine analogues with menin, we
27 co-crystallized menin in complex with **13**, which represents the most potent compound from this
28 series (**Table 2**) and solved a high-resolution crystal structure of the complex, **Figure 2a**,
29
30
31 **Supplementary Table 1**. The crystal structure revealed that the binding mode of **13** to menin is
32 similar as that observed for **MI-503**, with two hydrogen bonds (with Tyr276 and Trp341) and
33 hydrophobic interactions retained in **13** within the core structure preserved in both compounds
34
35
36
37
38
39
40
41
42
43
44
45
46
47
48
49
50
51
52
53
54
55
56
57
58
59
60

1
2
3 hydrophobic contacts with Val367 and Val371 on menin, while the other side of this ring in
4 exposed to the solvent, **Figure 2a**. In addition, the oxygen atom from the fluoroacetamide group
5 of **13** forms a hydrogen bond with the side chain of Arg330 (3.3 Å), while the fluoromethyl
6 group is involved in the hydrophobic interactions with the side chains of Cys329 and Arg330
7 with the fluorine atom approaching Cys329 and Gly326, **Figure 2a**. Overall, favorable
8 interactions of the fluoroacetamide group in **13** with menin result in the most pronounced activity
9 of this compound among all amide or sulfonamide derivatives, **Table 2, 3**. The crystal structure
10 also demonstrates limited space in the binding site to accommodate hydrophobic groups larger
11 than acetamide, reflected by the reduced activity of such analogs (e.g. compounds **12** and **14-17**,
12 **Table 2**). Overall, the crystal structure of menin in complex with **13** supports that both
13 hydrophobic contacts and hydrogen bond with Arg330 on menin contribute to the pronounced
14 inhibitory activity of this compound.
15
16
17
18
19
20
21
22
23
24
25
26
27
28
29
30
31
32

33 **Development of compound 28 as a highly potent menin-MLL inhibitor**

34
35 Exploring different saturated rings introduced at indole nitrogen led to the identification of **7**,
36 which demonstrated the most potent inhibitory activity for blocking the menin-MLL interaction
37 (IC₅₀ = 7.5 nM for the racemic mixture), **Table 1**. This compound harbors a morpholinone ring
38 introduced to the indole nitrogen through a methyl linker, **Table 1**. In addition to exhibiting the
39 most potent *in vitro* activity, compound **7** also demonstrated the most pronounced cell growth
40 inhibition in the MLL-AF9 leukemia cells (GI₅₀ = 50 nM), **Table 1**. To assess the activity of
41 individual enantiomers of this compound we synthesized both of them, resulting in **28** (*S*
42 enantiomer, **MI-1481**) and **29** (*R* enantiomer, **MI-1482**), **Table 4**. The *S* enantiomers (**28**)
43 demonstrated a ~2-fold improvement in inhibitory activity for blocking the menin-MLL
44
45
46
47
48
49
50
51
52
53
54
55
56
57
58
59
60

1
2
3 interaction ($IC_{50} = 3.6$ nM) over the racemic mixture (compound **7**), **Figure 3a**, **Table 4**. Thus,
4
5 **28** demonstrates about 10-fold increase in inhibitory activity over **MI-463** and **MI-503** (**Table 1**),
6
7 representing the most potent reversible menin-MLL inhibitor reported to date. In contrast, the *R*
8
9 enantiomer (compound **29**) demonstrated a ~35-fold reduction in inhibitory activity in blocking
10
11 the menin-MLL interaction ($IC_{50} = 123$ nM for **29**) as compared to **28**, **Figure 3a**, **Table 4**. Thus,
12
13 **28** and **29** provide a valuable pair of enantiomers with distinct inhibitory activity to study menin-
14
15 MLL inhibition in biological systems.
16
17
18
19
20

21 **Molecular basis of menin-MLL inhibition by compound 28**

22
23
24 To understand the molecular basis of the strong inhibition of the menin-MLL interaction
25
26 by **28**, we co-crystallized menin in complex with this compound, resulting in a high-resolution
27
28 crystal structure, **Supplementary Table 1**, **Figure 2b**. We found a similar interaction pattern of
29
30 **28** with menin to the one observed in the menin-**MI-503** complex for the structural fragment
31
32 retained in both compounds (e.g. hydrogen bonds with Tyr276 and Trp341 and similar pattern of
33
34 hydrophobic interactions), **Figure 1b**, **2b**. Again, the differences were found in the binding of
35
36 substituents introduced at indole nitrogen. Specifically, the methyl group linking indole with the
37
38 morpholinone ring in **28** is involved in the hydrophobic interactions with Glu363, Met322 and
39
40 Val 367, **Figure 2b**. Furthermore, one side of the morpholinone ring in **28** is involved in
41
42 hydrophobic contacts with the side chains of Glu363, Glu366 and Val367 on menin, while the
43
44 amino portion of the amide forms a short hydrogen bond (2.6 Å) with the carboxyl group of
45
46 Glu366 (**Figure 2b**). This hydrogen bond, which was not observed for the piperazine analogues
47
48 (e.g. in the menin-**13** complex), most likely contributes to the pronounced inhibitory activity of
49
50 **28**. The carbonyl carbon and the adjacent methylene group in **28** are engaged in the hydrophobic
51
52
53
54
55
56
57
58
59
60

1
2
3 contacts with Val371, while the ether oxygen is solvent exposed and does not form major
4 contacts with menin, **Figure 2b**. In contrast, the pyrazole ring introduced at the indole nitrogen
5 of **MI-503** is mostly solvent exposed, with one hydrogen bond formed with Glu366, **Figure 1b**.
6
7

8
9
10 To understand better the improvement in inhibitory activity for **28** over **MI-503** we
11 performed the bio-layer interferometry (BLI) studies and compared binding affinities of both
12 compounds to menin. This study demonstrated that the association rates to menin are similar for
13 both compounds, however, the dissociation rate is significantly slower for **28** over **MI-503**,
14 resulting in the K_d value of ~ 3 -fold improved for **28** ($K_d = 9$ nM) as compared to **MI-503** ($K_d =$
15 24 nM), **Supplementary Figure 2**. Furthermore, we have also performed structural analysis of
16 menin interactions with ligands by overlapped the crystal structures of menin in complex with:
17 the bi-valent MLL peptide encompassing both MBM1 and MBM2 motifs, **MI-503** and **28**,
18 **Figure 2c**. This analysis have revealed that both compounds occupy the same region of the
19 binding site on menin where MBM1 motif binds, however **28** approaches more closely the
20 region occupied by MBM2, particularly Arg24 from MLL, as compared to **MI-503**, **Figure 2c**.
21 Therefore, **28** might be able to more effectively displace the bi-valent MLL peptide from its
22 binding to menin likely due to stronger interference with the MBM2 portion of MLL, as reflected
23 by ~ 10 -fold improved inhibitory activity of **28** over **MI-503**. Overall, both structural data (e.g.
24 extensive interactions with menin and interference with the MBM2 motif) as well as binding
25 kinetics support **28** as a more effective inhibitor of the menin-MLL interaction over the previous
26 generation of menin-MLL inhibitors (e.g. **MI-503** or **MI-463**), **Tables 1, 4**. To better understand
27 the molecular basis of the differential inhibitory activity between both enantiomers of **7**, we also
28 solved the co-crystal structure of menin in complex with **29** (*R* enantiomer of **7**), **Figure 2d**,
29 **Supplementary Table 1**. The core structure of **29** binds to menin in the same way as observed
30
31
32
33
34
35
36
37
38
39
40
41
42
43
44
45
46
47
48
49
50
51
52
53
54
55
56
57
58
59
60

1
2
3 for **28**, but the orientation of the morpholinone ring in **29** is different from that of **28**, **Figure 2d**,
4 which results in significantly reduced contacts of this ring with menin. The most striking
5 difference in the binding mode of **29** and **28** is the lack of a hydrogen bond between the amide
6 nitrogen in **29** and the carboxyl group of Glu366 in menin, which is present when **28** binds to
7 menin, **Figure 2b,d**. Compound **29** also has limited hydrophobic contacts with menin as
8 compared to **28**, as **29** engages only a small portion of the morpholinone ring in the interactions
9 with Glu366, Val367 and Val371 on menin, **Figure 2d**. Overall, we concluded that limited
10 interactions of the morpholinone ring in **29** with menin, in particular the lack of a hydrogen bond
11 with Glu366, result in a 35-fold reduction in inhibitory activity of this compound to menin as
12 compared to **28**.
13
14
15
16
17
18
19
20
21
22
23
24
25
26
27

28 **Compound 28 demonstrates potent on target activity in MLL leukemia cells**

29
30 To assess whether potent inhibition of the menin-MLL interaction by **28** results in strong activity
31 of this compound in functional assays, we tested **28** in several leukemia cell lines. Importantly,
32 **28** markedly reduced cell growth of murine bone marrow cells transformed with MLL-AF9, with
33 a GI₅₀ value of 34 nM (**Table 4, Figure 3b**). In contrast, limited activity of this compound was
34 observed in murine bone marrow cells transformed with the control oncogenes Hoxa9/Meis1
35 (HM-2, GI₅₀ > 6 μM), **Figure 3b**. Thus, **28** demonstrated over 200-fold selectivity towards MLL
36 fusion protein transformed cells, **Table 4**, demonstrating substantial improvement in selectivity
37 over the previous generation of menin-MLL inhibitors (e.g. selectivity index, SI ~ 27 for **MI-503**
38 in MLL leukemia cells).¹² When tested in human MLL leukemia cell lines, **28** also showed
39 pronounced cell growth inhibition, with GI₅₀ values of 36 nM in MV4;11 (harboring MLL-AF4
40 fusion protein) and 61 nM in MOLM13 (harboring MLL-AF9), **Figure 3c**. Importantly, no
41
42
43
44
45
46
47
48
49
50
51
52
53
54
55
56
57
58
59
60

1
2
3 substantial cell growth inhibition was observed in the control human leukemia cell lines K562
4 and U937, which do not harbor MLL translocations ($GI_{50} > 6 \mu\text{M}$), **Figure 3c**. Therefore, **28**
5
6 shows the most pronounced activity in MLL leukemia cells among all reversible menin-MLL
7
8 inhibitors reported to date, **Tables 1-4**,^{10, 12} demonstrating ~7-10-fold improvement in the
9
10 activity in MLL leukemia cells over **MI-463** or **MI-503** (**Table 1**).¹⁰ As pointed out above, the
11
12 increased cellular activity of **28** is associated with ~10-fold improved inhibitory activity of this
13
14 compound in blocking the menin-MLL interaction as compared to **MI-463** or **MI-503**, **Table 1**,
15
16
17 **4**. In contrast, compound **29**, which represents the *R* enantiomer of **7**, showed limited activity in
18
19 MLL leukemia cells (over 16-fold weaker than **28**), **Figure 3d**, in agreement with the
20
21 substantially reduced inhibitory activity of **29**, **Table 4**.
22
23
24
25

26 To validate the on target activity of **28** in MLL leukemia cells, we assessed the effect of
27
28 this compound on the expression level of the MLL fusion target genes: *HOXA9*, *MEIS1* and
29
30 *DLX2*, all of which are required for the MLL-fusion protein mediated leukemogenesis. Six days
31
32 of treatment of the MV4;11 human MLL leukemia cells with **28** resulted in a substantial
33
34 downregulation of the MLL fusion protein target genes, with a strong reduction in the expression
35
36 level of *HOXA9* and *MEIS1* at 100 nM of **28**, **Figure 3e**. The effect of **28** on the expression level
37
38 of *DLX2* was even more pronounced, **Figure 3e**. Furthermore, marked upregulation of the
39
40 *ITGAM* differentiation marker was observed upon treatment of MV4;11 cells with **28** (**Figure**
41
42 **3e**), supporting reprogramming of these cells from primitive blasts to more mature blood cells.
43
44 Overall, **28** demonstrates a pronounced effect on the expression level of MLL fusion target
45
46 genes, which strongly supports the on target activity of this compound in MLL leukemia cells.
47
48
49
50
51
52
53

54 **Compound 28 strongly inhibits leukemia progression *in vivo***
55
56
57
58
59
60

1
2
3 We then performed pharmacokinetic (PK) studies in mice with **28** and found relatively high
4 exposure of this compound in blood plasma using i.v. (intravenous) and i.p. (intraperitoneal)
5 administration (**Supplementary Figure 3**), however, oral bioavailability of this compound was
6 low (<5%). Based on these results we selected i.p. as a way of administration of **28** for *in vivo*
7 efficacy studies. To establish a potential therapeutic value of **28**, we tested the effect of this
8 compound in a mice model of MLL leukemia. For this purpose, we utilized the
9 xenotransplantation model of the MLL leukemia with MV4;11-luc cells (expressing luciferase)
10 injected into the tail vein of NSG mice. Treatment with **28** (80 mg/kg, i.p., n = 8) or vehicle (n =
11 8) was initiated 13 days after transplantation of mice with the MV4;11 cells to account for a
12 compound effect in an advanced leukemia model, and was continued for 21 consecutive days.
13 No reduction in the body weight of mice was observed during the entire treatment period with
14 **28**, **Supplementary Figure 4**. To assess treatment efficacy, the bioluminescence level in mice
15 was measured at days 0, 7, 14 and 21 after initiating the treatment. Very pronounced (~75%) and
16 consistent reduction in the luciferase signal was observed over the course of the experiment upon
17 treatment of mice with **28** as compared to the vehicle treated mice, **Figure 4a,b**. These results
18 demonstrate the pronounced effect **28** on leukemia progression in an advanced model of MLL
19 leukemia.

20
21
22 To validate the on-target *in vivo* activity of **28** we performed gene expression studies in
23 bone marrow and spleen samples isolated from mice transplanted with MV4;11 cells and treated
24 with **28** or vehicle. Treatment with **28** was initiated 21 days after transplantation of mice with the
25 leukemic cells to account for the effect of **28** in advanced leukemia model. Compound **28** (or
26 vehicle) was administered for six consecutive days, followed by collection of the bone marrow
27 and spleen samples. Importantly, substantial reduction in the spleen weight and size was
28
29
30
31
32
33
34
35
36
37
38
39
40
41
42
43
44
45
46
47
48
49
50
51
52
53
54
55
56
57
58
59
60

1
2
3 observed for mice treated with **28** compared to the vehicle control, **Figure 4c**. Furthermore, the
4 level of leukemic blasts (human CD45+ cells) was very high (~75%) in the bone marrow cells
5 isolated from vehicle treated mice, which was indicative of advanced leukemia, while the level
6 of leukemic blasts was substantially reduced (to ~35%) in mice treated with **28**, **Figure 4d**. We
7 then performed gene expression studies in bone marrow and spleen samples isolated from mice
8 treated with **28** or vehicle using qRT-PCR and found that treatment with **28** resulted in a strong
9 reduction (2-5 fold) in the expression level of MLL fusion target genes *MEIS1* and *HOXA9*,
10 **Figure 4e**. Furthermore, an over 4-6-fold increase in the expression of *ITGAM* differentiation
11 marker was observed in the bone marrow and spleen samples upon treatment with **28**, **Figure 4e**.
12 Overall, the results from gene expression studies demonstrate pronounced, on-target activity of
13 **28** in the advanced mouse model of MLL leukemia, thus supporting the potential therapeutic
14 value of this compound.
15
16
17
18
19
20
21
22
23
24
25
26
27
28
29
30
31
32

33 Chemistry

34
35 Synthesis of compounds **3** and **4** was performed using the synthetic route shown in
36 **Scheme 1**. Two major intermediates: 5-formyl-4-methyl-1H-indole-2-carbonitrile (**30**) and *N*-
37 (piperidin-4-yl)-6-(2,2,2-trifluoroethyl)thieno[2,3-d]pyrimidin-4-amine (**33**) were obtained
38 according to the procedure described before.¹⁰ The alcohols **31a,b** were converted into mesylates
39 followed by the substitution with the aldehyde **30** in the presence of cesium carbonate, which
40 afforded aldehydes **32a,b**. (**Scheme 1**). Compounds **32a,b** were then used in the reductive
41 amination reaction with the secondary amine **33** utilizing sodium triacetoxyborohydride as the
42 reducing agent to afford compounds **34a,b**. Removal of the tert-butoxycarbonyl (Boc) group in
43 the presence of tin (IV) chloride resulted in compounds **3** and **4**. Compound **5** bearing the
44
45
46
47
48
49
50
51
52
53
54
55
56
57
58
59
60

1
2
3 morpholinone ring was obtained using the strategy depicted in **Scheme 2**. The 4-(2-
4 chloroethyl)morpholine (**35**) was used for the indole alkylation of aldehyde **30**, resulting in
5
6 compound **36**, **Scheme 2**. The reductive amination of aldehyde **36** with the amine **33** resulted in
7
8 compound **5**, **Scheme 2**.
9
10

11
12 The racemic mixtures of compounds **6** and **7** were prepared according to the synthetic
13 route presented in **Scheme 3**. The intermediates **39a** and **39b** were obtained using the methods
14 described before.³⁰⁻³¹ Briefly, the commercially available 3-amino-1,2-propanediol (**37a**) and
15 methyl 4-amino-3-hydroxybutanoate (**37b**) were subjected to acylation with the chloroacetic
16 acid, resulting in compounds **38a** and **38b**, respectively. Direct cyclisation of **38a** with potassium
17 *t*-butoxide afforded alcohol **39a**. Homologous alcohol **39b** was achieved by reduction of the ester
18 group in **38b** followed by the analogous cyclisation with potassium *t*-butoxide as a base (**Scheme**
19 **3**). The alcohols **39a,b** were then converted to the corresponding mesylates and used for
20 alkylation of the indol **30** to afford aldehydes **40a** and **40b**. Reductive amination reactions of the
21 intermediate **33** with aldehydes **40b** or **40a** led to the target compounds **6** and **7**, respectively
22 (**Scheme 3**).
23
24
25
26
27
28
29
30
31
32
33
34
35
36

37
38 The synthetic route for compounds **8** and **9** harboring the piperazine ring in the structure
39 is shown in **Scheme 4**. Briefly, both compounds were prepared from **3** using either formaline
40 (for **8**) or propionaldehyde (for **9**) in the reductive amination reaction, **Scheme 4**. The piperazine
41 and piperidine analogues **10-27** were obtained according to the synthetic strategy depicted in
42 **Scheme 5**. In general, the amide series (compounds **10-17** and **24-25**) was obtained by acylation
43 of the amines **3** or **4**. The formamides **10** and **24** were prepared by formylation of **3** or **4**,
44 respectively, with the methyl formate. The corresponding acyl chlorides were used to convert the
45 amine **3** into compounds **11**, **12** or **17** with DIPEA serving as a base, **Scheme 5**. The analogous
46
47
48
49
50
51
52
53
54
55
56
57
58
59
60

1
2
3 reaction was performed with the amine **4** to afford compound **25**. Synthesis of the amides
4
5 **13,14,16** was performed by utilizing the coupling reaction between the amine **3** and the
6
7 corresponding carboxylic acids in the presence of 2-(1H-Benzotriazole-1-yl)-1,1,3,3-
8
9 tetramethylammonium tetrafluoroborate (TBTU) serving as a condensing reagent, **Scheme 5**.
10
11 Compound **15** with the trifluoroacetyl moiety was prepared using the triflate anhydride as an
12
13 acylating agent. Alkylation of the nitrogen in the piperazine ring of **3** by the 2-
14
15 bromopropionamide led to the amine **18**. **Scheme 5**.
16
17
18

19
20 The sulfonamide series (compounds **19-21, 26**) was obtained using the sulfonylation
21
22 reactions with compounds **3** or **4** and the appropriate sulfonyl chlorides, **Scheme 5**. The two-step
23
24 synthetic approach was applied to afford compounds **22** and **27**. The benzyl
25
26 (chlorosulfonyl)carbamate was used for sulfonylation of the amines **3** or **4**, followed by the
27
28 cleavage of the Cbz-protected amino group performed with Pd/C and ammonium formate, which
29
30 led to sulfamides **22** or **27**, **Scheme 5**. Conversion of the amine **3** to compound **23** was achieved
31
32 using the methylsulfonyl chloride in the presence of DIPEA.
33
34

35
36 Synthesis of compounds **28** and **29**, which represent single enantiomers of **7**, was
37
38 performed by applying the same methodology as for compound **7**, **Scheme 3** through utilizing
39
40 the non-racemic 3-aminopropane-1,2-diols: **37a(S)** or **37a(R)**.
41
42
43

44 45 **Conclusions**

46
47 Identification of potent inhibitors targeting protein-protein interactions and optimization of their
48
49 drug-like properties represents a challenge as such compounds frequently have large molecular
50
51 weight, which is required for effective blocking of PPI interfaces.¹⁸⁻²⁰ This is particularly true for
52
53 compounds that target extended protein-protein interfaces, including inhibitors of the BCL-2
54
55
56
57

1
2
3 family of proteins ²⁶ and others.¹ On the other hand, recent FDA approval of the BCL-2 inhibitor
4 Venetoclax demonstrates that PPI inhibitors with large molecular weight (>800 Da) can serve as
5 valuable therapeutics. In the current study, we report optimization of the small molecule
6 inhibitors of the menin-MLL interaction, with the major goal of improving the potency and drug-
7 like properties of these compounds. The MLL binding site on menin is large (over 5,000 Å³ ⁹) as
8 menin binds long, bivalent MLL peptide (MLL₄₋₄₃). This suggests that compounds with large
9 molecular weight may be required for effective inhibition of the menin-MLL interaction.

10
11
12
13
14
15
16
17
18
19 Using the crystal structure of menin in complex with **MI-503** we designed, synthesized
20 and evaluated a series of new analogues by exploring various saturated rings that substitute
21 indole nitrogen in **MI-503**, **Tables 1-4**. The goal of this work was to increase the inhibitory
22 activity and metabolic stability of menin-MLL inhibitors by introducing substituents with
23 different physicochemical properties (e.g. charged versus uncharged substituents, hydrogen bond
24 donor or acceptor groups, etc.). These efforts resulted in compound **28**, which demonstrates very
25 potent inhibition of the menin-MLL interaction (IC₅₀ = 3.6 nM with MLL₄₋₄₃). Therefore, **28**
26 represents the most potent reversible small molecule inhibitor of the menin-MLL interaction
27 reported to date ^{10, 12}. About 10-fold improved inhibitory activity for **28** over previous generation
28 of reversible menin-MLL inhibitors (e.g. **MI-503**, **MI-463**) results from stronger binding affinity
29 of this compound to menin, but also likely from more pronounced overlap with MBM2 binding
30 to menin, as supported by the structural data, **Figure 2c**. Furthermore, **28** demonstrates stronger
31 effect (>8-fold) and better selectivity towards MLL leukemia cells than **MI-503**, and it has also
32 more pronounced effect on the target gene expression in mouse models of MLL leukemia,
33 **Figure 5E**.¹⁰ On the other hand, increased polarity of **28** (clogP value reduced) and increased
34 molecular weight (by ~30 Da) over **MI-503** (M_w = 597 Da for **28**) negatively affected oral
35
36
37
38
39
40
41
42
43
44
45
46
47
48
49
50
51
52
53
54
55
56
57
58
59
60

1
2
3 bioavailability of this compound. These results demonstrate the complexity of blocking bi-valent
4 protein-protein interactions with large molecular interfaces, where achievement of potent
5 inhibition requires effective interference with both motifs occupying different regions of the
6 binding site. The increase in the molecular weight of inhibitors targeting bi-valent PPIs (e.g. >
7 500 Da) can negatively affect their drug-like properties, making the lead optimization process
8 extensive and complex.
9

10
11
12
13
14
15
16
17 Importantly, strong *in vitro* inhibition induced by **28** correlates well with pronounced
18 activity of this compound in MLL leukemia cells ($GI_{50} = 30-60$ nM), which represents almost
19 10-fold improvement over **MI-503** or any other reversible menin-MLL inhibitor^{10, 12}. In
20 addition, compound **28** demonstrates high selectivity (>100-fold) and specific mechanism of
21 action in MLL leukemia cells. Furthermore, the pronounced effect of **28** in inhibiting leukemia
22 progression in the disseminated model of MLL leukemia combined with the on-target
23 mechanism of action *in vivo* make this compound a very attractive candidate compound for
24 further studies. During the preparation of this article, irreversible menin-MLL inhibitors with
25 distinct molecular scaffold were reported,³² but these compounds did not show stronger *in vitro*
26 inhibitory activity over **28** despite covalent binding to menin. Furthermore, biological activity of
27 these irreversible menin-MLL inhibitors, especially in the *in vivo* models of MLL leukemia, and
28 their potential off-target effects remain to be assessed.
29
30
31
32
33
34
35
36
37
38
39
40
41
42
43

44
45 Overall, compound **28** identified in this study represents a valuable molecule to further
46 investigate the role of menin-MLL interaction in normal and pathological states. This compound
47 may also lead to the development of new therapeutic agents for MLL leukemia and possibly
48 solid tumors, including prostate cancer¹³ Ewing sarcoma,¹⁴ HCC,¹⁶ and other tumors that may
49 rely on the intact menin-MLL interaction. Our work demonstrates that, despite challenges
50
51
52
53
54
55
56
57
58
59
60

1
2
3 associated with the development of potent PPI inhibitors targeting bi-valent protein-protein
4 interfaces, successful identification of such compounds is possible and can lead to valuable
5 chemical tools for the scientific community and potentially to new therapeutic agents.
6
7
8
9

10 11 12 **Experimental Section**

13 14 ***Expression and purification of menin***

15
16 The expression and purification of menin have been described previously.⁸⁻⁹ In order to generate
17 biotinylated menin, we introduced Avi-tag sequence (AAALEGLNDIFEAQKIEWHE)³³ to the C-
18 terminus of menin. Protein was co-expressed in *E. Coli* BL21 (DE3) cells with the construct encoding
19 BirA enzyme³³ and purified using the same protocol as for the intact menin.
20
21
22
23
24

25 26 ***Biochemical characterization of menin-MLL inhibitors***

27
28 Inhibition of the menin-MLL interaction by small molecules was assessed by fluorescence
29 polarization (FP) assay. The fluorescein-labeled MLL₄₋₄₃ peptide (FLSN-MLL₄₋₄₃) at 4 nM,
30 menin at 4 nM and varying concentrations of compounds were used for IC₅₀ determination in the
31 FP buffer (50 mM Tris, pH 7.5, 50 mM NaCl, 1 mM TCEP). The complex of menin with the
32 FLSN-MLL₄₋₄₃ peptide was incubated for 1h. Compounds (5% final DMSO concentration) were
33 then added to the menin-FLSN_MLL₄₋₄₃ complex and incubated for 3h before changes in
34 fluorescence polarization (mP values) were measured using the PHERAstar microplate reader
35 (BMG). The IC₅₀ values were calculated in Origin 7.0 (OriginLab) by plotting the mP values
36 measured for each compound as a function of compound concentration.
37
38
39
40
41
42
43
44
45
46
47

48 49 ***Bio-Layer Interferometry (BLI) binding assay***

50
51 BLI assay was performed in 96-well microplates at room temperature with continues shaking at
52 1000 rpm using the Octet Red 96 system (ForteBio, Menlo Park, CA, USA). Biotinylated menin
53 was bound on Super Streptavidin (SSA) biosensors (ForteBio) by dipping sensors into 200 nM
54
55
56
57

1
2
3 biotinylated menin in the assay buffer composed of 50 mM Tris, pH 7.5, 50 mM NaCl, 1 mM
4 TCEP, 0.05% BSA, 0.01% Tween-20 and 2% DMSO. Menin binding was performed for 600 s
5 followed by equilibration in the assay buffer for 1200 s. Compounds (**28** and **MI-503**) were used
6 at 150 and 200 nM concentrations and binding was performed for 600 s followed by 1200 s
7 dissociation. Data were fit globally and generated automatically by Octet User Software
8 (ForteBio, Inc.). Analysis of binding kinetics was performed in Prism (GraphPad Software, Inc.).
9 K_{obs} values were extracted using one phase association equation, and K_{off} values were extracted
10 using one phase decay equation. Subsequently, K_{on} was derived using $K_{obs} = K_{on} \times [Ligand] +$
11 K_{off} , where [Ligand] is a free ligand concentration in solution. K_D was calculated as K_{off}/K_{on} .
12
13
14
15
16
17
18
19
20
21
22
23

24 ***Crystallization of menin complexes with small molecule inhibitors***

25
26 For co-crystallization experiments 2.5 mg/mL menin was incubated with small molecule
27 inhibitors at 1:3 molar ratio. Crystals were obtained using the sitting drop technique at 10 °C by
28 applying the procedure described previously.⁹ Prior to data collection, crystals were transferred
29 into a cryo-solution containing 20% PEG550 MME and flash-frozen in liquid nitrogen.
30
31
32
33
34

35 ***Crystallographic data collection and structure determination***

36
37 Diffraction data for menin and menin complexes were collected at the 21-ID-D and 21-ID-F
38 beamlines at the Life Sciences Collaborative Access Team at the Advanced Photon Source. Data
39 were processed with HKL-2000.³⁴ Structures of the complexes were determined by molecular
40 replacement using MOLREP with the apo-structure of human menin (PDB code: 4GPQ) as a
41 search model in molecular replacement. The model was refined using REFMAC,³⁵ COOT³⁶,
42 CCP4 package³⁷ and PHENIX³⁸. Validation of the structures was performed using
43 MOLPROBITY³⁹ and ADIT.⁴⁰ Details of data processing and refinement are summarized in
44
45
46
47
48
49
50
51
52
53

54 **Supplementary Table 1.** Coordinates and structure factors for menin-inhibitor complexes have
55
56
57
58
59
60

1
2
3 been deposited in the Protein Data Bank under the following codes: 6BXH (menin-compound
4 **13**), 6BXY (menin-compound **28**), 6BY8 (menin-compound **29**).

7 *Viability assays*

8
9
10 The MLL-AF9, HM-2 and E2A-HLF transformed murine bone marrow cells (BMCs) were
11 prepared as described previously.⁴¹ MV4;11, MOLM-13, K562 and U937 cells were cultured in
12 RPMI-1640 medium with 10% FBS, 1% penicillin/streptomycin and NEAA (Non-essential
13 amino acid) solution. For viability assay, MOLM-13 (1×10^5 /mL), MV4;11 (1×10^5 /mL), K562
14 (1×10^5 /mL) and U937 (1×10^5 /mL) human leukemia cells as well as MLL-AF9, HM-2 and E2A-
15 HLF murine bone marrow cells (2.5×10^4 /mL) were plated (1 mL/well), treated with compounds
16 or 0.25% DMSO and cultured at 37 °C for 7 days. Media were changed at day four with viable
17 cell number restored to the original concentration and compounds were re-supplied. 100 μ L of
18 cell suspension were transferred to 96 well plates for each sample in quadruplicates. A Vybrant
19 MTT cell proliferation assay kit (Molecular Probes) was employed. Plates were read for
20 absorbance at 570 nm using a PHERAstar BMG microplate reader. The experiments were
21 performed 2-3 times in quadruplicated with calculation of mean and standard deviation for each
22 condition.

23 *Real-Time PCR*

24
25
26 Effect of **28** on the expression level of MLL fusion target genes was assessed by Real-time
27 quantitative PCR (qRT-PCR) using the protocol described previously.¹⁰

28 *Microsomal stability studies*

29
30
31 The metabolic stability was assessed using CD-1 mouse liver microsomes. 1 μ M compounds
32 were incubated with 1.3 mg/mL microsomes and 1.7 mM cofactor NADPH in 0.1 M phosphate
33 buffer (pH =7.4) containing 3.3 mM $MgCl_2$ at 37 °C. The DMSO concentration was less than
34
35
36
37
38
39
40
41
42
43
44
45
46
47
48
49
50
51
52
53
54
55
56
57
58
59
60

1
2
3 0.1% in the final incubation system. At 0, 3, 5, 10, 15, 30, 45 and 60 min of incubation, the
4
5 reactions were stopped by adding 3-fold excess of acetonitrile containing 100 ng/mL of internal
6
7 standard for quantification. The collected fractions were centrifuged at 3000 g for 20 min to
8
9 collect the supernatant for LC-MS/MS analysis, from which the amount of compound remaining
10
11 was determined. The natural log of the amount of compound remaining was plotted against time
12
13 to determine the disappearance rate and the half-life of tested compounds.
14
15

16 17 *Pharmacokinetic studies in mice*

18
19 All animal experiments in this study were approved by the University of Michigan Committee on
20
21 Use and Care of Animals and Unit for Laboratory Animal Medicine (ULAM).
22

23
24 The pharmacokinetics of **28** was determined in female C57BL/6 mice following intravenous (iv)
25
26 dosing at 15 mg/kg and 30 mg/kg for oral (po) and intraperitoneal (ip) dosing. For iv and po
27
28 administration, **28** was dissolved in the vehicle containing 25% (v/v) DMSO, 25% (v/v) PEG400
29
30 and 50% (v/v) PBS. For ip administration, **28** was dissolved in the vehicle containing 20% HP- β -
31
32 cyclodextrin and 5% Cremophor. Serial blood samples were collected over 7h, centrifuged at
33
34 15,000 rpm for 10 min and saved for analysis. Plasma concentrations of **28** were determined by
35
36 the LC-MS/MS method developed and validated for this study. The LC-MS/MS method
37
38 consisted of an Agilent 1200 HPLC system and chromatographic separation of **28** was achieved
39
40 using an Agilent Zorbax Extend-C18 column (5 cm x 2.1 mm, 3.5 μ m; Waters). An AB Sciex
41
42 QTrap 3200 mass spectrometer equipped with an electrospray ionization source (ABI-Sciex,
43
44 Toronto, Canada) in the positive-ion multiple reaction monitoring (MRM) mode was used for
45
46 detection. Pharmacokinetic parameters were calculated by noncompartmental methods using
47
48 WinNonlin® version 3.2 (Pharsight Corporation, Mountain View, CA, USA).
49
50
51

52 53 *In vivo efficacy studies*

1
2
3 All animal experiments in this study were approved by the University of Michigan Committee on
4 Use and Care of Animals and Unit for Laboratory Animal Medicine (ULAM).
5

6
7 For *in vivo* efficacy studies, 6 to 8-week-old female NSG mice (Jackson laboratory) were
8 intravenously injected with 1×10^7 luciferase-expressing MV4;11 cells. At day 13 post-
9 transplantaion, mice were split into vehicle and the treatment groups of 8 mice per group and
10 were treated for 21 consecutive days with once daily intraperitoneal injections of vehicle (20%
11 HP- β -cyclodextrin and 5% Cremophor) or 80 mg/kg of **28** dissolved in vehicle. Imaging of mice
12 was performed at days 0, 7, 14 and 21 of treatment with **28**. For imaging, mice were kept
13 anesthetized with Isoflurane, and luciferase at 50 mg/kg was administered by intraperitoneal
14 injection. Photonic emission was imaged using the *in Vivo* Imaging System BLI (IVIS, 200)
15 with total imaging time of 10 seconds for each mouse. Survival of mice was monitored to assess
16 treatment efficacy.
17
18
19
20
21
22
23
24
25
26
27
28
29

30 For the *in vivo* gene expression studies, 21 days after transplantation of mice with MV4;11 cells
31 mice were grouped into vehicle or compound **28** treatment groups ($n = 3$ / group), and the
32 treatment was initiated and continued for 6 consecutive days (80 mg/kg, *i.p.*, once daily). The
33 next day after completing the treatment mice were sacrificed and bone marrow samples were
34 isolated for gene expression studies by qRT-PCR.
35
36
37
38
39
40
41

42 ***Flow cytometric analysis of mice samples***

43
44 To assess levels of leukemia burden in the mice transplanted with leukemic cells, cells from bone
45 marrow, peripheral blood, and spleen were buffered with PBS and 1% FBS for flow cytometry
46 analysis. Red blood cells were lysed with ACK (Lonza). All flow cytometry experiments were
47 performed on a LSR II FACSCanto or FACSAria (BD Biosciences), and all data were analyzed
48 with FlowJo software (Tree Star, Inc.).
49
50
51
52
53
54
55
56
57

General Chemistry

All commercially available solvents and reagents were used without further preparation unless otherwise indicated. The ^1H and ^{13}C NMR data were taken on Bruker Avance III 600 MHz or Varian MR400. Chemical shifts are reported in ppm relative to tetramethylsilane or residual solvent signal. Some signals that overlapped with solvents were identified using ^1H - ^{13}C HSQC spectrum (multiplicity not known). The mass measurements were determined on a Micromass LCT time-of-flight mass spectrometer using positive mode and electrospray ionization. The exact mass measurements were determined on Agilent Q-TOF time-of-flight mass spectrometer using positive ion mode and electrospray ionization. Analytical TLC was performed on Merck TLC aluminum plates precoated with F₂₅₄ silica gel 60 (UV, 254 nm, and iodine). The purity analysis of final compounds was determined on Shimadzu Prominence HPLC system (20 series: binary pump, UV/vis at 254 nm, heated column compartment 28 °C), using Restek Ultra C18 (5 μm) 150 mm \times 4.6 mm column. LR-MS was recorder on Shimadzu LC-2020 system (DUIS-ESI). The solvents were programmed to run at gradient starting 20% CH₃CN in water to 80% during 8 min run. If not indicated, the purity of all final compounds was >95% as determined by HPLC via integration of UV spectra at 254 nm. Optical rotation was measured using Jasco P2000 polarimeter (path length = 100 mm). All final (unless indicated otherwise) compounds **1-29** were tested as hydrochloride salts. The general procedure for HCl salt formation: free base was dissolved in minimum volume of methanol followed by addition of 1 equiv of 1 M HCl in water and thorough drying. During NMR experiment, most of the hydrochloride salts of these compounds exist as a mixture of two forms in solution of either DMSO or MeOH with the approximate ratio of 10:1; NMR is reported for the major rotamer or a free base as indicated.

1
2
3 **4-methyl-1-(2-(piperazin-1-yl)ethyl)-5-((4-((6-(2,2,2-trifluoroethyl)thieno[2,3-d]pyrimidin-**
4 **4-yl)amino)piperidin-1-yl)methyl)-1H-indole-2-carbonitrile (3)**. To a stirred solution of *tert*-
5 butyl 4-(2-hydroxyethyl)piperazine-1-carboxylate (**31a**, 1 g 4.3 mmol) and trimethylamine (1.5
6 eq, 898 μ L, 6.45 mmol) in DCM (14 ml) methanesulfonyl chloride (1.2 eq, 399 μ L, 5.16 mmol)
7 was added dropwise at 0°C. Mixture was allowed to warm to the room temperature and stirred
8 for 3 h. The organic phase was diluted with DCM (40 mL) and washed with water, brine and
9 dried over sodium sulfate. Solvent was evaporated (partial decomposition was observed when
10 heated over 35°C during evaporation) and crude product (1.25 g) was used in the next step. The
11 5-formyl-4-methyl-1H-indole-2-carbonitrile (**30**, 300 mg, 1.63 mmol) was suspended in DMF
12 (3.2 mL) and cesium carbonate was added (1.63 g, 4.68 mmol, 3 eq). The *tert*-butyl 4-(2-
13 ((methylsulfonyl)oxy)ethyl)piperazine-1-carboxylate, from the previous step (753 mg, 2.45
14 mmol, 1.5 eq) was then added and resulting suspension was stirred at room temperature for 22 h.
15 Reaction was quenched with water and extracted with DCM (3x40 mL). Organic phase was
16 evaporated with silica gel and separated using flash chromatography (silica gel, hexanes:ethyl
17 acetate 3:1 to 1:1, v:v). 316 mg of compound *tert*-butyl 4-(2-(2-cyano-5-formyl-4-methyl-1H-
18 indol-1-yl)ethyl)piperazine-1-carboxylate (**32b**) was isolated (48% yield). MS (m/z) found for
19 [M+H⁺]: 397 Da. Compound **32b** (880 mg, 2.79 mmol, 1 eq) and amine **33** (1.01 g, 3.06 mmol,
20 1.1 eq) were then dissolved in DCM (28 mL). Triethylamine was added (1.6 mL, 4 eq) followed
21 by sodium triacetoxyborohydride (1.2 g, 5.6 mmol, 2 eq). Reaction was stirred overnight at room
22 temperature. Mixture was diluted with DCM (50 mL) and washed with 1M NaOH_{aq}. Organic
23 phase was dried over sodium sulfate and evaporated with silica gel. Purified using flash
24 chromatography (silica gel, dichloromethane:methanol with 5% ammonia, 0% to 5%, v:v). 1.2 g
25 of product **34b** (*tert*-butyl 4-(2-(2-cyano-4-methyl-5-((4-((6-(2,2,2-trifluoroethyl)thieno[2,3-
26
27
28
29
30
31
32
33
34
35
36
37
38
39
40
41
42
43
44
45
46
47
48
49
50
51
52
53
54
55
56
57
58
59
60

d]pyrimidin-4-yl)amino)piperidin-1-yl)methyl)-1H-indol-1-yl)ethyl)piperazine-1-carboxylate) was isolated (62% yield). ¹H NMR (600 MHz, CDCl₄/METHANOL-d₄) δ 8.29 (s, 1H), 7.31 - 7.39 (m, 2H), 7.17 - 7.24 (m, 2H), 4.34 (t, *J* = 6.2 Hz, 2H), 4.10 - 4.19 (m, 1H), 3.65 (q, *J* = 10.27 Hz, 2H), 3.61 - 3.70 (m, 2H), 3.33 - 3.39 (m, 4H), 2.91 - 3.10 (m, 2H), 2.72 (t, *J* = 6.42 Hz, 2H), 2.54 (s, 3H), 2.38 - 2.46 (m, 4H), 2.19 - 2.38 (m, 2H), 1.95 - 2.06 (m, 2H), 1.55 - 1.72 (m, 2H), 1.40 (s, 9H); MS (m/z) found for [M+H⁺]: 697 Da. Compound **34b** (180 mg, 0.26mmol) was then dissolved in acetonitrile (2.6 mL) and tin (IV) chloride (677 mg, 304 μL, 2.6 mmol, 10 eq) was added at 0°C. The reaction was stirred for 1h at room temperature and then cooled again to 0°C. Ammonia solution (30%_{aq}) was added slowly and DCM was evaporated. Water was added (2 mL) followed by tartaric acid (750 mg). The mixture was sonicated until the solution became clear. The product was extracted with DCM:MeOH (10:1). Purified on preparative TLC (silica gel, dichloromethane:methanol with 5% ammonia, 5%, v:v). 88 mg of compound **3** was isolated (57%). ¹H NMR (600 MHz, CHLOROFORM-d) δ 8.47 (s, 1H), 7.35 (d, *J* = 8.44 Hz, 1H), 7.18 (s, 1H), 7.14 - 7.17 (m, 1H), 7.10 (s, 1H), 5.21 (d, *J* = 7.70 Hz, 1H), 4.33 (t, *J* = 6.60 Hz, 2H), 4.14 - 4.29 (m, 1H), 3.57 - 3.68 (m, 4H), 2.87 - 2.97 (m, 6H), 2.66 - 2.74 (m, 2H), 2.54 (s, 3H), 2.46 - 2.53 (m, 4H), 2.22 - 2.30 (m, 2H), 2.04 - 2.12 (m, 2H), 1.53 - 1.65 (m, 2H); ¹³C NMR (151 MHz, CHLOROFORM-d) δ 166.8, 156.1, 154.3, 136.4, 131.2, 129.0, 128.6, 128.0, 127.3, 124.7 (*J* = 277 Hz) 118.6, 116.4, 114.0, 111.6, 109.8, 107.2, 60.1, 57.8, 53.9, 52.3, 51.3, 48.0, 45.5, 43.3, 35.7 (*J* = 32 Hz), 32.4, 15.1; HRMS (ESI): [M+H⁺] calculated 597.2736; found 597.2731.

4-methyl-1-(2-morpholinoethyl)-5-((4-((6-(2,2,2-trifluoroethyl)thieno[2,3-d]pyrimidin-4-yl)amino)piperidin-1-yl)methyl)-1H-indole-2-carbonitrile (5). Compound **30** (84 mg, 0.46 mmol, 1 eq) and 4-(2-chloroethyl)morpholine (**35**) (126 mg, 0.68 mmol, 1.5 eq) were dissolved

1
2
3 in DMF (0.92 mL). TBAI (85 mg, 0.23 mmol, 0.5 eq) was added followed by cesium carbonate
4 (905 mg, 1.76 mmol, 6 eq). The suspension was heated at 60°C for 1h. DMF was evaporated
5
6 with silica gel and product was isolated using flash chromatography (silica gel, hexane:ethyl
7
8 acetate, 1:1, v:v) to afford 63 mg of compound **36** (47% yield). Compound **36** (22 mg, 0.07
9
10 mmol) was then suspended in DCM (0.7 mL) and compound **33** (32 mg, 0.09 mmol, 1.2eq) and
11
12 triethylamine (20 μ L, 0.11 mmol, 1.4 eq) were added. The suspension was stirred for 15 min and
13
14 then sodium triacetoxyborohydride (23 mg, 0.11 mmol, 1.5 eq) was added. The reaction was
15
16 stirred overnight. DCM was added to dilute the solution and organic phase was washed with 1M
17
18 NaOH_{aq} and brine. DCM was evaporated and the product was recrystallized from MeOH
19
20 affording 30 mg of compound **5** (67% yield). ¹H NMR CD₃OD (600 MHz): δ 8.35 (s, 1H), 7.56
21
22 (m, 3H), 7.45 (s, 1H), 4.54 (m, 2H), 4.49 (m, 3H), 3.87 (q, J = 11 Hz, 2H), 3.65 (m, 6H), 2.79
23
24 (m, 2H), 2.70 (s, 3H), 2.53 (m, 4H), 2.35 (m, 2H), 1.99 (m, 2H). ¹³C NMR CD₃OD (150 MHz): δ
25
26 167.1, 157.7, 154.9, 138.8, 135.1, 130.6, 130.0, 128.8, 126.6 (q, J = 276 Hz), 121.9, 121.2,
27
28 118.3, 114.6, 113.4, 112.6, 110.6, 67.9, 59.0, 58.8, 55.0, 53.1, 47.2, 44.2, 35.9, 35.7 (q, J = 33
29
30 Hz), 30.1, 15.9. HRMS (ESI): [M+H⁺] calculated 598.2570; found 598.2573.

31
32
33 **4-methyl-1-(2-(4-propylpiperazin-1-yl)ethyl)-5-((4-((6-(2,2,2-trifluoroethyl)thieno[2,3-**
34
35 **d]pyrimidin-4-yl)amino)piperidin-1-yl)methyl)-1H-indole-2-carbonitrile (9)**. Compound **3**
36
37 (20 mg, 0.03 mmol, 1eq) and propionaldehyde (3 μ L, 0.034 mmol, 1.2 eq) were dissolved in
38
39 DCM (0.3 mL). After stirring for 15 min sodium triacetoxyborohydride (13 mg, 0.06 mmol, 2
40
41 eq) was added. The mixture was directly evaporated with silica gel and compound **9** (10 mg,
42
43 56% yield) was purified using flash chromatography (silica gel, dichloromethane:methanol with
44
45 5% ammonia_{aq}, 5%, v:v). ¹H NMR CD₃OD (600 MHz): δ 8.36 (s, 1H), 7.63 (m, 1H), 7.56 (m,
46
47 2H), 7.56 (m, 2H), 7.45 (s, 1H), 4.55 (m, 2H), 4.49 (m, 2H), 3.86 (q, J = 11 Hz, 2H), 3.62 (m,
48
49
50
51
52
53
54
55
56
57
58
59
60

2H), 3.49 (m, 2H), 3.06 (m, 5H), 2.84 (m, 2H), 2.70 (s, 3H), 2.55 (m, 2H), 2.34 (m, 2H), 2.04 (m, 2H), 1.76 (m, 2H), 1.00 (t, $J = 7.3$ Hz, 3H). ^{13}C NMR CD_3OD (150 MHz): δ 176.4, 166.6, 157.7, 154.7, 154.7, 138.7, 135.1, 130.8, 130.1, 128.7, 126.8 (q, $J = 276$ Hz), 121.8, 121.1, 118.2, 114.8, 113.3, 112.6, 110.4, 59.4, 58.8, 57.7, 53.3, 52.9, 51.3, 47.1, 44.4, 35.6 (q, $J = 33$ Hz), 29.9, 22.1, 18.5, 15.8, 11.1. HRMS (ESI): $[\text{M}+\text{H}^+]$ calculated 639.3200; found 639.3198.

1-(2-(4-formylpiperazin-1-yl)ethyl)-4-methyl-5-((4-((6-(2,2,2-trifluoroethyl)thieno[2,3-d]pyrimidin-4-yl)amino)piperidin-1-yl)methyl)-1H-indole-2-carbonitrile (10). Compound **3** (750 mg, 1.25 mmol) was dissolved in methyl formate (10 mL) and stirred overnight. Solvent was evaporated with silica gel and compound **10** (700 mg, 89% yield) was isolated using flash chromatography (silica gel, dichloromethane:methanol with 5% ammonia_{aq}, 5%, v:v). ^1H NMR CD_3OD (600 MHz): δ 8.34 (s, 1H), 7.98 (m, 1H), 7.61 (m, 1H), 7.55 (m, 2H), 7.45 (s, 1H), 4.55 (m, 2H), 4.49 (m, 3H), 3.86 (q, $J = 11$ Hz, 2H), 3.64 (m, 2H), 3.48 (m, 2H), 3.43 (m, 2H), 3.35 (m, 2H), 2.85 (m, 2H), 2.70 (s, 3H), 2.58 (m, 2H), 2.50 (m, 2H), 2.34 (m, 2H), 2.03 (m, 2H). ^{13}C NMR CD_3OD (150 MHz): δ 167.0, 163.2, 157.8, 154.9, 138.9, 135.2, 130.8, 130.1, 128.9, 126.8 (q, $J = 276$ Hz), 121.9, 121.2, 118.3, 114.7, 113.4, 112.6, 110.6, 59.0, 58.2, 54.9, 53.8, 53.0, 47.2, 46.7, 44.4, 40.9, 35.7 (q, $J = 33$ Hz), 30.1, 16.0. HRMS (ESI): $[\text{M}+\text{H}^+]$ calculated 625.2679; found 625.2682.

General procedure for synthesis of compounds 11 and 12. Compound **3** (20 mg, 0.03 mmol) was dissolved in DCM or AcCN (0.2 mL) and DIPEA (12 μL , 0.05 mmol) was added. Mixture was cooled to 0°C and corresponding acid chloride was added. Mixture was allowed to warm to the room temperature and was stirred until no starting material was detected by TLC (30 min).

1-(2-(4-acetylpiperazin-1-yl)ethyl)-4-methyl-5-((4-((6-(2,2,2-trifluoroethyl)thieno[2,3-d]pyrimidin-4-yl)amino)piperidin-1-yl)methyl)-1H-indole-2-carbonitrile (11). Reaction

1
2
3 carried out in AcCN with acetyl chloride. Isolated 16 mg (86% yield). ¹H NMR CD₃OD (600
4 MHz): δ 8.38 (s, 1H), 7.69 (m, 2H), 7.58 (s, 1H), 7.53 (s, 1H), 4.56 (m, 2H), 4.49 (m, 1H), 3.87
5
6 (q, *J* = 11 Hz, 2H), 3.80 (m, 2H), 3.63 (m, 2H), 3.35 (m, 2H), 3.19 (m, 4H), 2.71 (s, 3H), 2.34
7
8 (m, 2H), 2.13 (s, 3H), 2.04 (m, 2H). ¹³C NMR CD₃OD (150 MHz): 176.5, 171.9, 165.9, 157.7,
9
10 154.4, 139.0, 135.5, 131.3, 130.5, 128.9, 126.8 (q, *J* = 276 Hz), 122.0, 121.7, 118.3, 114.6,
11
12 114.2, 111.9, 110.6, 58.9, 56.5, 53.8, 53.6, 53.0, 47.4, 45.5, 42.0, 40.7, 35.7 (q, *J* = 33 Hz), 30.0,
13
14 27.4, 22.2, 21.1, 16.0. HRMS (ESI): [M+H⁺] calculated 639.2836; found 639.2841.

15
16
17
18
19 **4-methyl-1-(2-(4-propionylpiperazin-1-yl)ethyl)-5-((4-((6-(2,2,2-trifluoroethyl)thieno[2,3-**
20
21 **d]pyrimidin-4-yl)amino)piperidin-1-yl)methyl)-1H-indole-2-carbonitrile (12).** The reaction
22
23 was carried out in DCM with propionic acid chloride. Isolated 19 mg (99% yield). ¹H NMR
24
25 CD₃OD (600 MHz): δ 8.35 (s, 1H), 7.61 (m, 2H), 7.54 (s, 1H), 7.48 (s, 1H), 4.61 (m, 2H), 4.55
26
27 (m, 2H), 4.47 (m, 1H), 3.86 (q, *J* = 11 Hz, 2H), 3.62 (m, 2H), 3.60 (m, 2H), 3.35 (m, 2H), 2.70
28
29 (s, 3H), 2.34 (m, 2H), 2.40 (q, *J* = 7.6 Hz, 2H), 2.35 (m, 2H), 2.00 (m, 2H), 1.10 (t, *J* = 7.6 Hz,
30
31 3H). ¹³C NMR CD₃OD (150 MHz): 174.8, 166.8, 157.7, 154.7, 138.8, 135.2, 130.8, 130.0,
32
33 128.8, 126.8 (q, *J* = 276 Hz), 121.7, 121.2, 118.2, 114.4, 110.5, 58.8, 54.3, 54.0, 52.9, 47.1, 35.7
34
35 (q, *J* = 33 Hz), 30.0, 27.1, 15.8, 9.8. HRMS (ESI): [M+H⁺] calculated 653.2992; found 653.2989.

36
37
38
39
40 **General procedure for synthesis of compounds 13 and 14.** Compound **3** (30 mg, 0.05 mmol)
41
42 was dissolved in THF (0.5 mL). Fluoroacetic acid (3.1 μL, 0.06 mmol, 1.2 eq), difluoroacetic
43
44 acid (3.8 μL, 0.06 mmol, 1.2 eq) or 2-cyclopentylacetic acid (70 mg, 0.5 mmol, 1.1 eq) were
45
46 added followed by TBTU (22.8 mg, 0.07 mmol, 1.3 eq for **13** and **14**) or EDCI (11 mg, 0.06
47
48 mmol, 1.1 eq for **16**). Reaction was carried out at room temperature until the starting material
49
50 was not detected by LC-MS. (0.5-24h). Crude mixture was loaded on preparative TLC plate and
51
52 purified using DCM:methanol (20:1, v:v).
53
54
55
56
57

1
2
3 **1-(2-(4-(2-fluoroacetyl)piperazin-1-yl)ethyl)-4-methyl-5-((4-((6-(2,2,2-**
4 **trifluoroethyl)thieno[2,3-d]pyrimidin-4-yl)amino)piperidin-1-yl)methyl)-1H-indole-2-**
5 **carbonitrile (13).** Reaction time: 3h. Isolated 24 mg, 73 % yield. ¹H NMR CD₃OD (600 MHz):
6 δ 8.34 (s, 1H), 7.59 (m, 1H), 7.54 (m, 2H), 7.44 (s, 1H), 5.07 (d, *J* = 40 Hz, 2H), 4.54 (m, 2H),
7 4.47 (m, 3H), 3.86 (q, *J* = 11 Hz, 2H), 3.63 (m, 2H), 3.53 (m, 2H), 3.35 (m, 2H), 2.77 (m, 2H),
8 2.70 (s, 3H), 2.50 (m, 2H), 2.45 (m, 2H), 2.34 (m, 2H), 1.99 (m, 2H). ¹³C NMR CD₃OD (150
9 MHz): δ 168.2 (d, *J* = 40 Hz), 167.3, 158.0, 155.1, 139.0, 135.3, 130.8, 130.2, 129.0, 126.9 (q, *J*
10 = 276 Hz), 122.0, 121.3, 118.4, 114.9, 113.4, 112.9, 110.7, 80.5 (d, *J* = 40 Hz), 59.1, 58.5, 54.5,
11 54.2, 53.2, 47.4, 45.5, 44.8, 43.1, 35.7 (q, *J* = 33 Hz), 30.2, 16.1. HRMS (ESI): [M+H⁺]
12 calculated 657.2742; found 657.2745.
13
14

15 **1-(2-(4-(2,2-difluoroacetyl)piperazin-1-yl)ethyl)-4-methyl-5-((4-((6-(2,2,2-**
16 **trifluoroethyl)thieno[2,3-d]pyrimidin-4-yl)amino)piperidin-1-yl)methyl)-1H-indole-2-**
17 **carbonitrile (14).** Reaction time: 24h. Purified two times on the prep-TLC plate isolated 15 mg
18 (32%) ¹H NMR CD₃OD (600 MHz): δ 8.34 (s, 1H), 7.56 (m, 3H), 7.43 (s, 1H), 6.43 (t, *J* = 53
19 Hz, 1H), 4.47 (m, 5H), 3.86 (q, *J* = 11 Hz, 2H), 3.56 (m, 2H), 3.23 (m, 2H), 2.77 (m, 2H), 2.69
20 (s, 3H), 2.52 (m, 2H), 2.47 (m, 2H), 2.30 (m, 2H), 2.00 (m, 2H). ¹³C NMR CD₃OD (150 MHz): δ
21 167.2, 162.6 (d, *J* = 25 Hz), 162.5, 157.9, 155.0, 138.8, 135.0, 130.6, 130.1, 130.1, 128.9, 126.9
22 (q, *J* = 276 Hz), 121.9, 118.3, 114.8, 113.2, 112.7, 111.4, 110.4, 109.8, 108.2, 58.3, 54.5, 54.0,
23 46.2, 44.7, 43.7, 39.0, 35.7 (q, *J* = 33 Hz), 15.9. HRMS (ESI): [M+H⁺] calculated 675.2647;
24 found 675.2643.
25
26

27 **4-methyl-1-(2-(4-(2,2,2-trifluoroacetyl)piperazin-1-yl)ethyl)-5-((4-((6-(2,2,2-**
28 **trifluoroethyl)thieno[2,3-d]pyrimidin-4-yl)amino)piperidin-1-yl)methyl)-1H-indole-2-**
29 **carbonitrile (15).** Compound **3** (30 mg, 0.05 mmol) was dissolved in DCM (0.25 ml) and cooled
30
31
32
33
34
35
36
37
38
39
40
41
42
43
44
45
46
47
48
49

1
2
3 to 0°C. The triflate anhydride (7 μ L, 0.05 mmol) in DCM (0.25 mL) was added at 0°C. The
4
5 mixture was warmed to room temperature and solvents were evaporated with silica gel.
6
7 Compound **15** (21 mg, 60% yield) was purified using flash chromatography (silica gel,
8
9 DCM:methanol) ^1H NMR CD_3OD (600 MHz): δ 8.35 (s, 1H), 7.55(m, 3H), 7.43 (s, 1H), 4.50
10
11 (m, 5H), 3.85 (q, J = 11 Hz, 2H), 3.61 (m, 4H), 2.83 (m, 2H), 2.70 (s, 3H), 2.57 (m, 4H), 2.33
12
13 (m, 2H), 2.00 (m, 2H). ^{13}C NMR CD_3OD (150 MHz): δ 166.6, 157.7, 154.7, 138.8, 135.2, 130.6,
14
15 130.1, 128.8, 121.8, 121.1, 118.2, 114.6, 113.3, 112.6, 110.5, 58.9, 58.0, 54.2, 53.7, 52.9, 47.1,
16
17 46.8, 44.3, 35.7 (m), 30.0, 15.8; HRMS (ESI): $[\text{M}+\text{H}^+]$ calculated 693.2553; found 693.2558.

18
19
20
21
22 **1-(2-(4-(2-cyclopentylacetyl)piperazin-1-yl)ethyl)-4-methyl-5-((4-((6-(2,2,2-**
23
24 **trifluoroethyl)thieno[2,3-d]pyrimidin-4-yl)amino)piperidin-1-yl)methyl)-1H-indole-2-**
25
26 **carbonitrile (16).** Compound **16** was prepared using the same general procedure as described
27
28 for compounds **13** and **14**. Reaction time: 30 min. Isolated 19 mg, 54% yield. ^1H NMR (600
29
30 MHz, METHANOL-d_4) δ 8.36 (s, 1H), 7.55 – 7.62 (m, 3H), 7.45 (s, 1H), 4.50 – 4.60 (m, 2H),
31
32 4.45 - 4.53 (m, 3H), 3.88 (q, J = 10.6 Hz, 2H), 3.63 (d, J = 12.8 Hz, 2H), 3.49 - 3.57 (m, 4H),
33
34 3.30 – 3.43 (m, 2H, overlapped with the residual methanol signal), 2.78 (t, J = 5.5Hz, 2H), 2.72
35
36 (s, 3H), 2.50 (t, J = 5.14 Hz, 2H), 2.42 (t, J = 5.14 Hz, 2H), 2.39 (d, J = 7.34 Hz, 2H), 2.27 - 2.37
37
38 (m, 2H), 2.13 – 2.24 (m, 1H), 1.94 - 2.10 (m, 2H), 1.77 - 1.87 (m, 2H), 1.62 - 1.69 (m, 2H), 1.52
39
40 - 1.61 (m, 2H), 1.14 - 1.25 (m, 2H); ^{13}C NMR (151 MHz, METHANOL-d_4) δ 173.8, 167.1,
41
42 157.7, 154.9, 138.8, 135.0, 130.5, 130.0, 128.8, 126.6 (J = 277 Hz), 121.9, 121.2, 118.2, 114.6,
43
44 113.2, 112.6, 110.5, 58.9, 58.3, 54.7, 54.3, 52.9, 47.0, 44.6, 42.8, 39.9, 38.2, 35.7 (J = 32 Hz),
45
46 33.5, 30.0, 25.8, 15.8; HRMS (ESI): $[\text{M}+\text{H}^+]$ calculated 707.3462; found 707.3466.

47
48
49
50
51
52 **1-(2-(4-(3-cyclopentylpropanoyl)piperazin-1-yl)ethyl)-4-methyl-5-((4-((6-(2,2,2-**
53
54 **trifluoroethyl)thieno[2,3-d]pyrimidin-4-yl)amino)piperidin-1-yl)methyl)-1H-indole-2-**
55
56

carbonitrile (17). Compound **17** was prepared using the same synthetic procedure as described for compounds **11** and **12**. The reaction was carried out in DCM with 3-cyclopentylpropanoyl chloride. Reaction time: 30 min. Isolated 13 mg, 52% yield. ^1H NMR (600 MHz, METHANOL- d_4) δ 8.36 (s, 1H), 7.50 – 7.64 (m, 3H), 7.44 (s, 1H), 4.48 (t, J = 5.9 Hz, 2H), 4.33 - 4.47 (m, 3H), 3.88 (q, J = 10.6 Hz, 2H), 3.48 - 3.60 (m, 6H), 3.10 – 3.24 (m, 2H), 2.78 (t, J = 5.9 Hz, 2H), 2.70 (s, 3H), 2.48 – 2.54 (m, 2H), 2.41 – 2.45 (m, 2H), 2.36 – 2.40 (m, 2H), 2.26 - 2.33 (m, 2H), 2.21 – 2.26 (m, 1H), 1.93 - 2.12 (m, 2H), 1.77 - 1.86 (m, 2H), 1.62 - 1.69 (m, 2H), 1.51 - 1.61 (m, 4H), 1.08 - 1.19 (m, 2H); ^{13}C NMR (151 MHz, METHANOL- d_4) δ 179.5, 174.3, 167.1, 157.7, 154.9, 138.7, 134.6, 130.5, 129.9, 128.8, 126.6 (J = 276.20 Hz) 121.8, 118.2, 114.7, 113.1, 112.4, 110.2, 58.3, 54.7, 54.2, 47.0, 44.6, 42.8, 41.1, 35.7 (J = 31.9 Hz), 35.9, 33.5, 33.5, 33.4, 33.3, 32.9, 26.1, 15.7; HRMS (ESI): $[\text{M}+\text{H}^+]$ calculated 721.3618; found 721.3619.

2-(4-(2-(2-cyano-4-methyl-5-((4-((6-(2,2,2-trifluoroethyl)thieno[2,3-*d*]pyrimidin-4-yl)amino)piperidin-1-yl)methyl)-1*H*-indol-1-yl)ethyl)piperazin-1-yl)propanamide (18).

Compound **3** (57 mg, 0.1 mmol) was dissolved in DCM (0.5 mL) and 2-bromopropionamide (7 mg, 0.5eq) was added. After 24h the reaction was diluted with water (despite the presence of starting bromide) and extracted with DCM:MeOH (10:1, v:v). Compound **18** was purified using preparative TLC (silica gel, DCM:MeOH:NH₄OH, 10:1:0.05, v:v:v). 12 mg (18% yield) of the product was isolated. ^1H NMR (600 MHz, METHANOL- d_4) δ 8.33 (s, 1H), 7.55 (s, 1H), 7.46 - 7.54 (m, 2H), 7.40 (s, 1H), 4.45 (t, J = 6.2 Hz, 2H), 4.37 - 4.43 (m, 1H), 4.29 - 4.36 (m, 2H), 3.85 (q, J = 10.6 Hz, 2H), 3.47 (d, J = 12.8 Hz, 2H), 2.97 - 3.15 (m, 3H), 2.72 - 2.80 (m, 2H), 2.66 (s, 3H) 2.61 - 2.69 (m, 2H), 2.49 - 2.61 (m, 6H), 2.21 - 2.30 (m, 2H), 1.87 - 2.03 (m, 2H), 1.24 (d, J = 6.97 Hz, 3H); ^{13}C NMR (151 MHz, METHANOL- d_4) δ 178.4, 167.0, 157.7, 154.9, 138.6, 134.4, 130.5, 129.8, 128.7, 126.4 (J = 276.2 Hz), 123.20, 121.8, 118.2, 114.6, 113.1,

112.1, 110.1; 65.2, 59.2, 58.3, 54.2, 52.8, 51.0, 47.5, 44.4, 35.8 ($J = 31.8$ Hz), 30.8, 30.3, 15.7, 14.3; HRMS (ESI): $[M+H^+]$ calculated 668.3107; found 668.3098

General procedure for synthesis of compounds 19, 20 and 21. Compound **3** (1 eq), DIPEA (1.5 eq) were dissolved in DCM (6 ml/mmol). At 0°C the corresponding sulfonyl or sulfamoyl chloride (1 eq) was added and reaction was left to warm to the room temperature. The crude reaction was loaded on the silica gel column and purified using DCM:methanol.

4-methyl-1-(2-(4-(methylsulfonyl)piperazin-1-yl)ethyl)-5-((4-((6-(2,2,2-trifluoroethyl)thieno[2,3-d]pyrimidin-4-yl)amino)piperidin-1-yl)methyl)-1H-indole-2-carbonitrile (19). The reaction was performed with the methanesulfonyl chloride. Isolated 13 mg, 58% yield. 1H NMR CD_3OD (600 MHz): δ 8.36 (s, 1H), 7.59 (m, 2H), 7.54 (s, 1H), 7.46 (s, 1H), 4.55 (m, 4H), 4.47 (m, 1H), 3.86 (q, $J = 11$ Hz, 2H), 3.63 (m, 2H), 3.34 (m, 2H), 3.25 (m, 4H), 2.94 (m, 2H), 2.84 (s, 3H), 2.73 (m, 4H), 2.70 (s, 3H), 2.4 (m, 2H), 2.00 (m, 2H). ^{13}C NMR CD_3OD (150 MHz): δ 166.8, 157.8, 154.8, 138.9, 135.3, 130.9, 130.2, 128.9, 126.8 (q, $J = 276$ Hz), 121.9, 121.3, 118.3, 114.6, 113.7, 112.5, 110.6, 59.0, 57.7, 53.9, 53.0, 47.3, 46.6, 44.0, 35.7 (q, $J = 33$ Hz), 34.9, 30.1, 15.9. HRMS (ESI): $[M+H^+]$ calculated 675.2506; found 675.2503.

4-methyl-1-(2-(4-(ethylsulfonyl)piperazin-1-yl)ethyl)-5-((4-((6-(2,2,2-trifluoroethyl)thieno[2,3-d]pyrimidin-4-yl)amino)piperidin-1-yl)methyl)-1H-indole-2-carbonitrile (20). The reaction was performed with the ethanesulfonyl chloride. Isolated 20 mg, 58% yield. 1H NMR CD_3OD (600 MHz): δ 8.34 (s, 1H), 7.60 (m, 1H), 7.54 (m, 2H), 7.44 (s, 1H), 4.54 (m, 2H), 4.49 (m, 3H), 3.86 (q, $J = 11$ Hz, 2H), 3.63 (m, 2H), 3.34 (m, 2H), 3.26 (m, 4H), 3.02 (q, $J = 7.6$ Hz, 2H), 2.85 (m, 2H), 2.70 (s, 3H), 2.60 (m, 4H), 2.34 (m, 2H), 2.01 (m, 2H). ^{13}C NMR CD_3OD (150 MHz): δ 167.2, 157.9, 155.1, 139.0, 135.4, 130.9, 130.3, 129.0, 126.8 (q, $J = 276$ Hz), 122.0, 121.3, 118.4, 114.9, 113.6, 112.8, 110.7, 59.1, 58.2, 54.4, 53.2,

1
2
3 47.4, 46.8, 44.9, 44.5, 35.9 (q, $J = 33$ Hz), 30.2, 16.1, 8.3. HRMS (ESI): $[M+H]^+$ calculated
4 689.2662; found 689.2658.
5
6

7 **4-methyl-5-((4-((6-(2,2,2-trifluoroethyl)thieno[2,3-d]pyrimidin-4-yl)amino)piperidin-1-**
8 **yl)methyl)-1-(2-(4-((trifluoromethyl)sulfonyl)piperazin-1-yl)ethyl)-1H-indole-2-carbonitrile**
9 **(21)**. Trifluoromethanesulfonyl chloride was added to the reaction mixture at -78°C . Isolated 9
10 mg, 25% yield. ^1H NMR CD_3OD (600 MHz): δ 8.34 (s, 1H), 7.54 (m, 3H), 7.43 (s, 1H), 4.46
11 (m, 2H), 4.42 (m, 3H), 3.86 (q, $J = 11$ Hz, 2H), 3.53 (m, 2H), 3.45 (m, 2H), 3.19 (m, 4H), 2.80
12 (m, 2H), 2.68 (s, 3H), 2.55 (m, 4H), 2.28 (m, 2H), 1.97 (m, 2H). ^{13}C NMR CD_3OD (150 MHz): δ
13 167.0, 157.7, 154.9, 138.6, 134.7, 130.5, 129.9, 128.8, 126.8 (q, $J = 276$ Hz), 122.6, 121.8,
14 120.5, 118.2, 114.8, 113.1, 112.5, 110.2, 58.1, 54.0, 44.5, 35.6 (q, $J = 33$ Hz), 15.7. HRMS
15 (ESI): $[M+H]^+$ calculated 729.2223; found 729.2218.
16
17
18
19
20
21
22
23
24
25
26
27

28 **4-(2-(2-cyano-4-methyl-5-((4-((6-(2,2,2-trifluoroethyl)thieno[2,3-d]pyrimidin-4-**
29 **yl)amino)piperidin-1-yl)methyl)-1H-indol-1-yl)ethyl)piperazine-1-sulfonamide (22)**.
30

31 Compound **3** (59 mg, 0.1 mmol) and DIPEA (25 μL , 0.15 mmol, 1.5 eq) was dissolved in DCM
32 (1 mL). Benzyl (chlorosulfonyl)carbamate, CbzNHSO₂Cl (26 mg, 0.11 mmol, 1.1 eq), prepared
33 as described before⁴² was then added and reaction was carried out at room temperature for 30
34 min. Crude mixture was loaded on preparative TLC plate and Cbz-protected compound **22** was
35 purified (silica gel, DCM:MeOH:NH₃OH, 10:1:0.5 v:v:v). The product was then dissolved in
36 MeOH (2.25mL) and Pd/C (6 mg) and ammonium formate (9 mg, 0.13 mmol, 4 eq) were added.
37 The mixture was heated at 60°C for 12 h. Mixture was filtered through Celite and evaporated.
38 Purified using preparative TLC (silica gel, DCM:MeOH:NH₃OH, 10:1:0.5 v:v:v). 5.6 mg (8%
39 yield) of compound **22** was isolated. ^1H NMR CD_3OD (600 MHz): δ 8.51 (s, 1H), 7.76 (m, 1H),
40 7.67 (m, 2H), 7.58 (s, 1H), 4.56 (m, 4H), 4.42 (m, 3H), 3.92 (q, $J = 11$ Hz, 2H), 3.63 (m, 4H),
41
42
43
44
45
46
47
48
49
50
51
52
53
54
55
56
57

1
2
3 3.58 (m, 2H), 3.51 (m, 4H), 3.35 (m, 2H), 2.71 (s, 3H), 2.34 (m, 2H), 2.08 (m, 2H). ¹³C NMR
4 CD₃OD (150 MHz): δ 157.7, 153.7, 152.7, 139.1, 135.6, 131.6, 129.9, 129.7, 129.5, 129.0, 126.6
5
6 (q, *J* = 276 Hz), 122.3, 121.8, 118.5, 115.1, 114.0, 111.6, 110.6, 69.2, 63.3, 58.9, 55.6, 53.1,
7
8 52.9, 47.8, 45.1, 41.1, 35.5 (q, *J* = 33 Hz), 33.2, 30.9, 29.9, 26.2, 23.9, 16.0. HRMS (ESI):
9
10 [M+H⁺] calculated 676.2458; found 676.2463.

11
12
13
14
15 **4-(2-(2-cyano-4-methyl-5-((4-((6-(2,2,2-trifluoroethyl)thieno[2,3-d]pyrimidin-4-**
16
17 **yl)amino)piperidin-1-yl)methyl)-1H-indol-1-yl)ethyl)-N-methylpiperazine-1-sulfonamide**

18
19 **(23, tested as a free base).** Compound **23** was prepared using a general synthetic procedure as
20 described for compounds **19-21**. Reaction performed with the methylsulfamoyl chloride added to
21 the reaction mixture at the room temperature. Isolated 11 mg, 23% yield. ¹H NMR CD₃OD (600
22 MHz): δ 8.30 (s, 1H), 7.52 (s, 1H), 7.39 (m, 3H), 4.41 (m, 2H), 4.19 (m, 1H), 3.83 (q, *J* = 11 Hz,
23 2H), 3.76 (m, 2H), 3.12 (m, 4H), 3.07 (m, 2H), 2.75 (m, 2H), 2.61 (s, 3H), 2.59 (s, 3H), 2.51 (m,
24 4H), 2.39 (m, 2H), 2.03 (m, 2H). ¹³C NMR CD₃OD (150 MHz): δ 166.9, 157.9, 155.1, 138.2,
25
26 132.9, 130.5, 129.7, 129.6, 128.9, 126.8 (q, *J* = 276 Hz), 122.0, 118.3, 115.2, 112.8, 111.5,
27
28 109.2, 60.7, 58.3, 54.0, 53.8, 47.2, 44.5, 35.5 (q, *J* = 33 Hz), 32.3, 30.9, 29.7, 15.5, 15.5. HRMS
29
30 (ESI): [M+H⁺] calculated 690.2615; found 690.2611.

31
32
33
34
35
36
37
38
39
40 **(S)-4methyl-1-((5-oxomorpholin-2-yl)methyl)-5-((4-((6-(2,2,2-trifluoroethyl)thieno[2,3-**
41
42 **d]pyrimidin-4-yl)amino)piperidin-1-yl)methyl)-1H-indole-2-carbonitrile (28):** (S)-3-
43
44 aminopropane-1,2-diol (**37a**, 5 g, 55 mmol, 1 eq) was dissolved in methanol (20 ml) and the
45 solution was diluted by AcCN (60 ml) and trimethylamine was added, stirred and cooled at -20
46 °C. Chloroacetyl chloride was added slowly into the reaction mixture over 1 h and the
47 temperature was controlled to -15°C. The reaction mixture was slowly warmed to -10°C and
48 stirred for 1 h, then warmed to the room temperature and stirred overnight. Solvents were
49
50
51
52
53
54
55
56
57
58
59
60

1
2
3 removed and the residue was washed by ethyl acetate (800 mL), filtered and concentrated to give
4 the desired compound (*S*)-**38a**. (*S*)-2-chloro-*N*-(2,3-dihydroxypropyl)acetamide, (*S*)-**38a**, from
5 the previous step (2.0 g, 12 mmol) in *t*-amyl alcohol (32 ml) was added dropwise to the solution
6 of *t*-BuOK (4.7 g, 42 mmol, 3.5 eq) in *t*-amyl alcohol (45 mL) at the room temperature for 2.5 h.
7 The mixture was stirred for an additional 1 h. 1M HCl_{aq} (15 ml) was added to the mixture (to
8 adjust pH to ~2) and the mixture was stirred for additional 30 min. Solvents were removed and
9 the (*S*)-6-(hydroxymethyl)morpholin-3-one (*S*)-**39a** was purified using column chromatography
10 (silica gel, hexane:ethyl acetate then DCM:MeOH, 0-10% v:v). ¹H NMR (600 MHz, DMSO-*d*₆)
11 δ 7.90 (br. s., 1H), 4.82 (t, J = 5.69 Hz, 1H), 3.92 - 4.10 (m, 2H), 3.60 - 3.71 (m, 1H), 3.45 - 3.53
12 (m, 1H), 3.36 - 3.45 (m, 1H), 3.18 (td, J = 3.85, 12.10 Hz, 1H), 3.02 - 3.13 (m, 1H). Compound
13 (*S*)-**39a** (1 g, 7.6 mmol) was dissolved in DCM (12 mL) and TEA (1.4 mL, 9.9 mmol, 1.3 eq)
14 was added. Mixture was cooled to 0°C and methanesulfonyl chloride (823 μL, 9.9 mmol, 1.3 eq)
15 was added dropwise. The mixture was warmed to the room temperature and stirred overnight.
16 Solvent was evaporated and the residue was purified using column chromatography (silica gel,
17 DCM:MeOH, 0-10% v:v) providing 1.2 g of the (*S*)-(5-oxomorpholin-2-yl)methyl
18 methanesulfonate, which was directly used in the next step. The mesylate from the previous step
19 (1.2 g) was dissolved in DMA (22 mL) and cesium carbonate (7.5 g, 22.8 mmol, 4 eq) and
20 compound **30** (1.1 g, 5.7 mmol, 1 eq) were added. Mixture was stirred at 105°C for 4 h. After
21 cooling to the room temperature, ethyl acetate (150 ml) was added along with water (3x15 mL).
22 Organic phase was then separated and concentrated. The residue was purified using column
23 chromatography (silica gel, DCM:MeOH, 0-10% v:v) resulting in 420 mg of compound (*S*)-**40a**,
24 (*S*)-5-formyl-4-methyl-1-((5-oxomorpholin-2-yl)methyl)-1H-indole-2-carbonitrile, MS (m/z) found for
25 [M+AcCN+H⁺]: 339 Da. Compound (*S*)-**40a** (400 mg, 1.4 mmol) was dissolved in THF (48 mL)
26
27
28
29
30
31
32
33
34
35
36
37
38
39
40
41
42
43
44
45
46
47
48
49
50
51
52
53
54
55
56
57
58
59
60

1
2
3 followed by addition of compound **33** (638 mg, 2.0 mmol, 1.5 eq) and acetic acid (116 μ L).
4
5 Resulting mixture was stirred at 50°C for 30min, then cooled to the room temperature. Sodium
6
7 triacetoxyborohydride (572 mg, 2.69 mmol, 2 eq) was then added and the mixture was stirred
8
9 for 5 h at 50°C. Cooled mixture was then partitioned between EtOAc (60 mL) and 1M NaOH_{aq}
10
11 (25 mL). Organic phase was concentrated and product was purified by column chromatography
12
13 (silica gel, DCM:MeOH, 0-10% v:v). 520 mg (65% yield) of compound **28** was obtained. ¹H
14
15 NMR (600 MHz, DMSO-d₆) δ 10.68 (br. s., 1H), 8.38 (s, 1H), 8.20 – 8.29 (m, 1H), 8.00 – 8.03
16
17 (m, 1H), 7.76 - 7.81 (m, 1H), 7.75 (bs, 1H), 7.62 - 7.66 (m, 2H), 4.57 - 4.62 (m, 1H), 4.31 - 4.45
18
19 (m, 4H), 4.01 - 4.10 (m, 3H), 4.00 (d, J = 16.4 Hz, 1H), 3.89 (d, J = 16.5 Hz, 1H), 3.35 - 3.47 (m,
20
21 3H, overlapped with water), 3.21 - 3.32 (m, 2H), 3.18 (t, J = 11.37 Hz, 1H), 2.64 (s, 3H), 2.01 -
22
23 2.14 (m, 4H); ¹³C NMR (151 MHz, DMSO-d₆) δ 166.7, 155.7, 153.4, 137.3, 133.3, 130.0, 127.2,
24
25 126.5, 125.4 (J = 277 Hz) 121.5, 120.4, 116.2, 113.5, 113.2, 110.2, 109.3, 71.5, 66.9, 56.1, 50.6,
26
27 50.5, 46.8, 45.7, 42.7, 33.8 (J = 31 Hz), 28.2, 15.5; ¹H NMR (600 MHz, METHANOL-d₄) δ
28
29 8.41 (s, 1H), 7.57 - 7.67 (m, 3H), 7.49 (s, 1H), 4.61 (dd, J = 2.75, 15.22 Hz, 1H), 4.56 (s, 2H),
30
31 4.47 - 4.54 (m, 2H), 4.14 - 4.21 (m, 1H), 4.15 (AB, d, J = 16.51 Hz, 1H), 4.00 (AB, d, J = 16.51
32
33 Hz, 1H), 3.83 - 3.93 (m, 2H), 3.65 (d, J = 11.74 Hz, 2H), 3.48 (dd, J = 2.38, 12.29 Hz, 1H), 3.33
34
35 - 3.41 (m, 3H, partially overlapped with MeOH), 2.71 (s, 3H), 2.35 (bd, J = 13.20 Hz, 2H), 2.06
36
37 (q, J = 12.47 Hz, 2H); ¹³C NMR (151 MHz, METHANOL-d₄) δ 170.6, 165.1, 157.6, 153.9,
38
39 139.6, 135.0, 130.8, 130.5, 128.6, 126.6 (J = 276 Hz), 125.6, 121.9, 121.2, 118.3, 114.2, 114.0,
40
41 112.5, 73.3, 68.0, 58.8, 52.9, 52.9, 48.2, 47.3, 44.4, 35.6 (J = 32 Hz), 29.9, 15.8; $[\alpha]_D^{24}$ -17.5 (c
42
43 1.0, MeOH); HR-MS (ESI): $[M+H]^+$ calculated 598.2212, found 598.2208.
44
45
46
47
48
49
50
51
52
53
54
55
56
57
58
59
60

Synthesis of compounds **4**, **6**, **7**, **8**, **24**, **25**, **26**, **27**, **29** was outsourced to the contract research organization (CRO). These compounds were prepared using the general methodology presented in **Schemes 1**, **3**, **4**, **5**. Final compounds were characterized in-house and the purity was confirmed by HPLC before their biological activity was evaluated.

4-methyl-1-(2-(piperidin-4-yl)ethyl)-5-((4-((6-(2,2,2-trifluoroethyl)thieno[2,3-d]pyrimidin-4-yl)amino)piperidin-1-yl)methyl)-1H-indole-2-carbonitrile (4). ^1H NMR (600 MHz, DMSO- d_6) δ 11.02 (br. s., 1H), 9.08 (br. s., 1H), 8.90 (br. s., 1H), 8.79 (br. s., 1H), 8.49 (s, 1H), 7.74 - 7.91 (m, 2H), 7.65 (s, 1H), 7.57 (d, $J = 8.80$ Hz, 1H), 4.31 - 4.47 (m, 5H), 4.08 (q, $J = 10.88$ Hz, 2H), 3.41 (d, $J = 11.37$ Hz, 2H), 3.18 - 3.30 (m, 4H), 2.80 (q, $J = 11.74$ Hz, 2H), 2.65 (s, 3H), 2.04 - 2.22 (m, 4H), 1.88 (d, $J = 12.84$ Hz, 2H), 1.70 (q, $J = 6.72$ Hz, 2H), 1.55 - 1.65 (m, 1H), 1.36 - 1.48 (m, 2H) ^{13}C NMR (151 MHz, DMSO- d_6) δ 155.2, 151.6, 136.8, 133.5, 130.2, 129.9, 128.3, 126.6, 125.4 ($J = 276$ Hz), 121.7, 120.3, 116.5, 113.5, 113.1, 108.8, 108.8, 56.0, 50.4, 46.2, 42.8, 42.7, 35.9, 33.7 ($J = 31$ Hz) 30.7, 28.0, 28.0, 15.6; HRMS (ESI): $[\text{M}+\text{H}^+]$ calculated 596.2783; found 596.2776.

4-methyl-1-(2-(5-oxomorpholin-2-yl)ethyl)-5-((4-((6-(2,2,2-trifluoroethyl)thieno[2,3-d]pyrimidin-4-yl)amino)piperidin-1-yl)methyl)-1H-indole-2-carbonitrile (6). ^1H NMR (600 MHz, DMSO- d_6) δ 10.91 (br. s., 1H), 8.72 - 8.88 (m, 1H), 8.43 - 8.59 (m, 1H), 7.91 - 7.98 (m, 1H), 7.86 (s, 1H), 7.82 (d, $J = 8.80$ Hz, 1H), 7.65 (s, 1H), 7.53 (d, $J = 8.80$ Hz, 1H), 4.33 - 4.57 (m, 5H), 4.09 (q, $J = 11.0$ Hz, 2H), 4.05 (d, $J = 16.1$ Hz, 1H), 3.92 (d, $J = 16.1$ Hz, 1H), 3.49 - 3.58 (m, 1H), 3.36 - 3.46 (m, 2H), 3.19 - 3.30 (m, 2H), 3.11 - 3.18 (m, 1H), 3.02 - 3.10 (m, 1H), 2.65 (s, 3H), 2.06 - 2.26 (m, 4H), 1.99 - 2.07 (m, 1H), 1.85 - 1.95 (m, 1H); ^{13}C NMR (151 MHz, DMSO- d_6) δ 167.0, 155.3, 151.6, 136.9, 133.5, 130.1, 128.3, 126.6, 125.4 ($J = 277$ Hz), 121.7,

1
2
3 120.3, 116.5, 113.4, 113.1, 109.1, 108.8, 70.0, 66.8, 56.0, 50.5, 50.4, 46.2, 44.9, 41.6, 33.7 ($J =$
4 31 Hz), 32.3, 28.0, 15.6 HRMS (ESI): $[M+H^+]$ calculated 612.2369; found 612.2369.

5
6
7 **4-methyl-1-((5-oxomorpholin-2-yl)methyl)-5-((4-((6-(2,2,2-trifluoroethyl)thieno[2,3-**
8 **d]pyrimidin-4-yl)amino)piperidin-1-yl)methyl)-1H-indole-2-carbonitrile (7);** 1H NMR (600
9 MHz, DMSO- d_6) δ 10.67 (br. s., 1H), 8.52 - 8.63 (m, 1H), 8.45 (s, 1H), 8.01 (d, $J = 3.67$ Hz,
10 1H), 7.74 - 7.83 (m, 2H), 7.59 - 7.67 (m, 2H), 4.59 (dd, $J = 2.75, 15.22$ Hz, 1H), 4.33 - 4.47 (m,
11 4H), 4.03 - 4.14 (m, 3H), 3.99 (d, $J = 16.1$ Hz, 1H), 3.89 (d, $J = 16.5$ Hz, 1H), 3.36 - 3.47 (m,
12 3H), 3.21 - 3.33 (m, 2H), 3.18 (t, $J = 11.37$ Hz, 1H), 2.64 (s, 3H), 2.03 - 2.24 (m, 4H); ^{13}C NMR
13 (151 MHz, DMSO- d_6) δ 166.7, 155.5, 152.4, 137.4, 133.3, 130.0, 127.9, 126.6, 125.4 ($J =$
14 277Hz) 121.6, 120.4, 116.4, 113.5, 113.2, 110.2, 109.3, 71.5, 66.9, 56.1, 50.6, 50.5, 46.8, 46.0,
15 42.7, 33.7 ($J = 31$ Hz), 28.1, 15.5; HRMS (ESI): $[M+H^+]$ calculated 598.2212; found 598.2205.

16
17
18
19
20
21
22
23
24
25
26
27
28 **4-methyl-1-(2-(4-propylpiperazin-1-yl)methyl)-5-((4-((6-(2,2,2-trifluoroethyl)thieno[2,3-**
29 **d]pyrimidin-4-yl)amino)piperidin-1-yl)methyl)-1H-indole-2-carbonitrile (8)** 1H NMR (600
30 MHz, DMSO- d_6) δ 10.66 (bs, 1H), 8.38 (s, 1H), 8.25 (d, $J = 6.60$ Hz, 1H), 7.78 (d, $J = 8.80$ Hz,
31 1H), 7.74 (s, 1H), 7.58 - 7.70 (m, 2H), 4.50 (m, 2H), 4.40 (d, $J = 5.14$ Hz, 2H), 4.31 - 4.39 (m,
32 1H), 4.05 (q, $J = 11.13$ Hz, 2H), signals overlapped with water: 3.39 (HSQC), 3.36 (HSQC),
33 3.20 - 3.29 (m, 2H), 3.02 - 3.15 (m, 2H), 2.93 - 3.02 (m, 2H), 2.80 - 2.90 (m, 2H), 2.75 (s, 3H),
34 2.64 (s, 3H), 2.01 - 2.22 (m, 4H); ^{13}C NMR (151 MHz, DMSO- d_6) δ 155.6, 136.8, 133.4, 130.0,
35 126.6, 121.4, 116.2, 109.0, 69.1, 56.7 (HSQC) 56.1, 52.0, 50.6, 49.3, 45.8, 42.7 (HSQC), 41.9,
36 33.6, 28.2, 15.5; HRMS (ESI): $[M+H^+]$ calculated 611.2892; found 611.2873.

37
38
39
40
41
42
43
44
45
46
47
48
49
50 **1-(2-(1-formylpiperidin-4-yl)ethyl)-4-methyl-5-((4-((6-(2,2,2-trifluoroethyl)thieno[2,3-**
51 **d]pyrimidin-4-yl)amino)piperidin-1-yl)methyl)-1H-indole-2-carbonitrile (24);** 1H NMR (600
52 MHz, DMSO- d_6) δ 10.42 (br. s., 1H), 8.36 - 8.43 (m, 1H), 8.22 (d, $J = 7.34$ Hz, 1H), 7.96 (s,
53 54 55 56 57 58 59 60

1
2
3 1H), 7.71-7.77 (m, 2H), 7.65 (s, 1H), 7.58 (d, $J = 8.80$ Hz, 1H), 4.37 - 4.45 (m, 4H), 4.29 - 4.36
4 (m, 1H), 4.13 (d, $J = 13.20$ Hz, 1H), 4.05 (q, $J = 11.00$ Hz, 2H), 3.66 (d, $J = 13.20$ Hz, 1H), 3.42
5
6 (m, 2H, HSQC, overlapped with water) 3.20 - 3.29 (m, 2H), 2.94 - 3.03 (m, 1H), 2.64 (s, 3H),
7
8 2.54 - 2.61 (m, 1H), 2.08 - 2.20 (m, 2H), 1.96 - 2.07 (m, 2H), 1.73 - 1.84 (m, 2H), 1.71 (q, $J =$
9
10 6.97 Hz, 2H), 1.52 - 1.62 (m, 1H), 0.96 - 1.16 (m, 2H); ^{13}C NMR (151 MHz, DMSO- d_6) δ 160.6,
11
12 155.7, 153.3, 136.8, 133.5, 130.0, 127.3, 126.6, 125.5 ($J = 277$ Hz), 121.4, 120.3, 116.2, 113.5,
13
14 113.1, 108.9, 108.9, 56.2, 50.6, 45.7, 44.8, 42.8, 38.8, 36.2, 33.8 ($J = 30$ Hz), 33.2, 32.1, 30.8,
15
16 28.2, 15.5; HRMS (ESI): $[\text{M}+\text{Na}^+]$ calculated 646.2552; found 646.2544.

17
18
19
20
21
22 **1-(2-(1-acetylpiperidin-4-yl)ethyl)-4-methyl-5-((4-((6-(2,2,2-trifluoroethyl)thieno[2,3-**
23
24 **d]pyrimidin-4-yl)amino)piperidin-1-yl)methyl)-1H-indole-2-carbonitrile (25).** ^1H NMR (600
25
26 MHz, DMSO- d_6) δ 10.22 (bs, 1H), 8.36 (s, 1H), 8.11 (d, $J = 6.97$ Hz, 1H), 7.69 - 7.74 (m, 2H),
27
28 7.65 (s, 1H), 7.58 (d, $J = 8.80$ Hz, 1H), 4.36 - 4.46 (m, 4H), 4.30 - 4.35 (m, 2H), 4.05 (q, $J = 10.9$
29
30 Hz, 2H), 3.78 (d, $J = 13.2$ Hz, 1H), 2.97 (t, $J = 13.2$ Hz, 1H), 2.63 (s, 3H), 2.44 - 2.49 (m, 1H),
31
32 2.10-2.15 (m, 2H), 1.97 (s, 3H), 1.92 - 2.02 (m, 2H), 1.76 (d, $J = 13.2$ Hz, 1H), 1.66 - 1.74 (m,
33
34 3H), 1.48 - 1.57 (m, 1H), 1.15 (m, 1H), 0.96 - 1.07 (m, 1H); HSQC (^1H - ^{13}C): signals overlapped
35
36 with water: 3.43 (CH_2), 3.25 (CH_2); ^{13}C NMR (151 MHz, DMSO- d_6) δ 167.8, 165.6, 155.7,
37
38 153.7, 136.8, 133.5, 130.0, 127.2, 126.6, 125.50 ($J = 277\text{Hz}$), 121.4, 120.2, 116.9, 116.2, 113.5,
39
40 113.0, 108.9 56.3, 50.7, 45.7, 45.6, 42.9, 40.8, 36.2, 33.8 ($J = 32$ Hz), 32.9, 32.0, 31.3, 28.3,
41
42 21.2, 15.5 HRMS (ESI): $[\text{M}+\text{Na}^+]$ calculated 660.2703; found 660.2699.

43
44
45
46
47 **4-methyl-1-(2-(1-(methylsulfonyl)piperidin-4-yl)ethyl)-5-((4-((6-(2,2,2-**
48
49 **trifluoroethyl)thieno[2,3-d]pyrimidin-4-yl)-amino)piperidin-1-yl)methyl)-1H-indole-2-**
50
51 **carbonitrile (26)** ^1H NMR (600 MHz, DMSO- d_6) δ 10.75 (bs, 1H), 8.60 (bs, 1H), 8.46 (s, 1H),
52
53 7.81 (s, 1H), 7.79 (d, $J = 8.80$ Hz, 1H), 7.65 (s, 1H), 7.58 (d, $J = 8.80$ Hz, 1H), 4.32 - 4.45 (m,
54
55
56
57
58
59
60

1
2
3 5H), 4.08 (q, $J = 11.00$ Hz, 2H), 3.54 (d, $J = 12.1$ Hz, 2H), 3.42 (d, $J = 12.1$ Hz, 2H), 3.20 - 3.31
4 (m, 2H), 2.83 (s, 3H), 2.65 - 2.69 (m, 2H), 2.64 (s, 3H), 2.04 - 2.24 (m, 4H), 1.79 - 1.87 (m, 2H),
5
6 1.69 - 1.78 (m, 2H), 1.40 (m, 1H), 1.22 - 1.30 (m, 2H) ^{13}C NMR (151 MHz, DMSO- d_6) δ 155.4,
7
8 152.2, 136.8, 133.5, 130.1, 126.6, 126.4, 121.6, 120.3, 116.4, 113.5, 113.1, 108.9, 108.9, 108.9,
9
10 56.1, 50.5, 46.1, 45.3, 42.8, 35.9, 34.1, 33.7 ($J = 30$ Hz), 32.1, 30.9, 28.1, 15.5; HRMS (ESI):
11
12 [M+H $^+$] calculated 674.2559; found 674.2548.

13
14
15
16
17 **4-(2-(2-cyano-4-methyl-5-((4-((6-(2,2,2-trifluoroethyl)thieno[2,3-d]pyrimidin-4-yl)amino-**
18
19 **)piperidin-1-yl)methyl)-1H-indol-1-yl)ethyl)piperidine-1-sulfonamide (27).** ^1H NMR (600
20
21 MHz, DMSO- d_6) δ 10.58 (bs, 1H), 8.42 (s, 1H), 8.34 - 8.41 (m, 1H), 7.73 - 7.83 (m, 2H), 7.65 (s,
22
23 1H), 7.58 (d, $J = 8.80$ Hz, 1H), 6.65 (br. s., 2H), 4.32 - 4.46 (m, 5H), 4.06 (q, $J = 11.13$ Hz, 2H),
24
25 3.38 - 3.47 (m, 4H), 3.17 - 3.35 (m, 2H), 2.64 (s, 3H), 2.44 - 2.48 (m, 2H), 2.02 - 2.21 (m, 4H),
26
27 1.77 - 1.88 (m, 2H), 1.66 - 1.75 (m, 2H), 1.30 - 1.40 (m, 1H), 1.19 - 1.30 (m, 2H); ^{13}C NMR (151
28
29 MHz, DMSO- d_6) δ 155.6, 152.8, 136.8, 133.5, 130.0, 127.6, 126.6, 126.4, 124.5, 121.5, 120.3,
30
31 116.3, 113.5, 113.1, 108.9, 56.1, 50.6, 45.9, 42.9, 40.1, 36.0, 33.75 ($J = 31\text{Hz}$), 32.3, 30.6, 28.2,
32
33 15.5; HRMS (ESI): [M+H $^+$] calculated 675.2511; found 675.2505.

34
35
36
37
38 **(R)-4-methyl-1-((5-oxomorpholin-2-yl)methyl)-5-((4-((6-(2,2,2-trifluoroethyl)thieno[2,3-**
39
40 **d]pyrimidin-4-yl)amino)piperidin-1-yl)methyl)-1H-indole-2-carbonitrile (29)** ^1H NMR (600
41
42 MHz, DMSO- d_6) δ 10.68 (br. s., 1H), 8.48 - 8.56 (m, 1H), 8.44 (s, 1H), 8.01 (d, $J = 3.67$ Hz,
43
44 1H), 7.75 - 7.81 (m, 2H), 7.61 - 7.66 (m, 2H), 4.59 (dd, $J = 2.75, 15.22$ Hz, 1H), 4.33 - 4.45 (m,
45
46 4H), 4.03 - 4.11 (m, 3H), 4.00 (d, $J = 16.5$ Hz, 1H), 3.89 (d, $J = 16.5$ Hz, 1H), 3.37 - 3.47 (m,
47
48 3H), 3.21 - 3.32 (m, 2H), 3.18 (t, $J = 11.37$ Hz, 1H), 2.64 (s, 3H), 2.06 - 2.15 (m, 4H); ^{13}C NMR
49
50 (151 MHz, DMSO- d_6) δ 166.7, 155.5, 152.5, 137.4, 133.3, 130.0, 127.8, 126.4, 125.4 ($J =$
51
52 276Hz) 121.6, 120.4, 116.4, 113.5, 113.2, 110.2, 109.3, 71.5, 66.9, 56.1, 50.6, 50.5, 46.8, 46.0,
53
54
55
56
57
58
59
60

1
2
3 42.7, 33.7 ($J = 32$ Hz), 28.1, 15.5; $[\alpha]_D^{24}$ 18.1 (c 1.0, MeOH); HR-MS (ESI): $[M+H^+]$ calculated
4
5 598.2212, found 598.2207.
6
7
8
9

10 **Acknowledgements**

11
12 This work was funded by the National Institute of Health (NIH) grants R01 (1R01CA160467) to
13
14 J.G., R01 (1R01CA200660) and R01 (1R01CA201204) to J.G., a Leukemia and Lymphoma
15
16 Society LLS Scholar (1215-14) to J.G., LLS TAP (Therapy Acceleration Program) to J.G.,
17
18 American Cancer Society Research Scholar grant RSG-13-130-01-CDD to J.G., and the
19
20 Department of Pathology, University of Michigan. Use of the Advanced Photon Source was
21
22 supported by the US Department of Energy, Office of Science, Office of Basic Energy Sciences
23
24 under contract number DE-AC02-06CH11357. Use of the LS-CAT Sector 21 was supported by
25
26 the Michigan Economic Development Corporation and the Michigan Technology Tri-Corridor
27
28 for the support of this research program (grant 085P1000817). The mouse work was performed
29
30 under oversight of UCUCA at the University of Michigan.
31
32
33
34
35
36
37

38 **Author information notes**

39
40 Corresponding author: Jolanta Grembecka, University of Michigan, Department of Pathology,
41
42 1150 W. Medical Center Dr, MSRBI, Rm 4510D, Ann Arbor, MI, 48109; e-mail:
43
44 jolantag@umich.edu, Tel. 734-615-9319, Fax. 734-763-8764
45
46

47 **Author Contributions:** [#] D. B. and S. K. contributed equally to this work.
48
49
50

51 **Accession Codes**

52
53
54
55
56
57

The atomic coordinate files have been deposited in PDB with the PDB codes: 6BXH (menin-compound **13**), 6BXY (menin-compound **28**), 6BY8 (menin-compound **29**).

Abbreviations used

FP, Fluorescence Polarization; MLL, Mixed Lineage Leukemia; PPI, Protein-Protein Interaction; NEAA, Non-essential amino acids; FBS, fetal bovine serum; AcCN, acetonitrile; AcOH, acetic acid; DIPEA, N,N-Diisopropylethylamine; EDCI, N-(3-Dimethylaminopropyl)-N'-ethylcarbodiimide hydrochloride; TEA, trimethylamine; TBTU, O-(Benzotriazol-1-yl)-N,N,N',N'-tetramethyluronium tetrafluoroborate; TBAI, Tetrabutylammonium iodide.

Supporting Information

Supplementary Table 1 with crystallography data, **Supplementary Figure 1** with the K_d results from the FP assay for MLL₄₋₄₃ binding to menin, **Supplementary Figure 2** with BLI studies for menin-MLL inhibitors, **Supplementary Figure 3** with PK results for **28** and **Supplementary Figure 4** with mice body weight from *in vivo* efficacy studies with **28**. Molecular Formula Strings are available. This material is available free of charge via the Internet at <http://pubs.acs.org>.

Conflict of interest. The authors declare the following competing financial interest(s): Drs. Grembecka and Cierpicki receive research support from Kura Oncology, Inc. They have also an equity ownership in the company. Other coauthors declare no potential conflict of interest.

References

1. Cierpicki, T.; Grembecka, J. Challenges and opportunities in targeting the menin-MLL interaction. *Future Med. Chem.* **2014**, *6* (4), 447-462.
2. Yokoyama, A.; Somervaille, T. C.; Smith, K. S.; Rozenblatt-Rosen, O.; Meyerson, M.; Cleary, M. L. The menin tumor suppressor protein is an essential oncogenic cofactor for MLL-associated leukemogenesis. *Cell.* **2005**, *123* (2), 207-218.
3. Marschalek, R. Mechanisms of leukemogenesis by MLL fusion proteins. *Br. J. Haematol.* **2011**, *152* (2), 141-154.
4. Dimartino, J. F.; Cleary, M. L. Mll rearrangements in haematological malignancies: lessons from clinical and biological studies. *Br. J. Haematol.* **1999**, *106* (3), 614-626.
5. Popovic, R.; Zeleznik-Le, N. J. MLL: how complex does it get? *J. Cell Biochem.* **2005**, *95* (2), 234-242.
6. Caslini, C.; Yang, Z.; El-Osta, M.; Milne, T. A.; Slany, R. K.; Hess, J. L. Interaction of MLL amino terminal sequences with menin is required for transformation. *Cancer Res.* **2007**, *67* (15), 7275-7283.
7. Yokoyama, A.; Cleary, M. L. Menin critically links MLL proteins with LEDGF on cancer-associated target genes. *Cancer Cell.* **2008**, *14* (1), 36-46.
8. Grembecka, J.; He, S.; Shi, A.; Purohit, T.; Muntean, A. G.; Sorenson, R. J.; Showalter, H. D.; Murai, M. J.; Belcher, A. M.; Hartley, T.; Hess, J. L.; Cierpicki, T. Menin-MLL inhibitors reverse oncogenic activity of MLL fusion proteins in leukemia. *Nat. Chem. Biol.* **2012**, *8* (3), 277-284.

- 1
2
3 9. Shi, A.; Murai, M. J.; He, S.; Lund, G.; Hartley, T.; Purohit, T.; Reddy, G.; Chruszcz, M.;
4 Grembecka, J.; Cierpicki, T. Structural insights into inhibition of the bivalent menin-MLL
5 interaction by small molecules in leukemia. *Blood* **2012**, *120* (23), 4461-4469.
6
7
8
9
10 10. Borkin, D.; He, S.; Miao, H.; Kempinska, K.; Pollock, J.; Chase, J.; Purohit, T.; Malik,
11 B.; Zhao, T.; Wang, J.; Wen, B.; Zong, H.; Jones, M.; Danet-Desnoyers, G.; Guzman, M. L.;
12 Talpaz, M.; Bixby, D. L.; Sun, D.; Hess, J. L.; Muntean, A. G.; Maillard, I.; Cierpicki, T.;
13 Grembecka, J. Pharmacologic inhibition of the Menin-MLL interaction blocks progression of
14 MLL leukemia in vivo. *Cancer Cell* **2015**, *27* (4), 589-602.
15
16
17
18
19 11. He, S.; Senter, T. J.; Pollock, J.; Han, C.; Upadhyay, S. K.; Purohit, T.; Gogliotti, R. D.;
20 Lindsley, C. W.; Cierpicki, T.; Stauffer, S. R.; Grembecka, J. High-affinity small-molecule
21 inhibitors of the menin-mixed lineage leukemia (MLL) interaction closely mimic a natural
22 protein-protein interaction. *J. Med. Chem.* **2014**, *57* (4), 1543-1556.
23
24
25
26
27
28
29
30 12. Borkin, D.; Pollock, J.; Kempinska, K.; Purohit, T.; Li, X.; Wen, B.; Zhao, T.; Miao, H.;
31 Shukla, S.; He, M.; Sun, D.; Cierpicki, T.; Grembecka, J. Property focused structure-based
32 optimization of small molecule inhibitors of the protein-protein interaction between menin and
33 Mixed Lineage Leukemia (MLL). *J. Med. Chem.* **2016**, *59* (3), 892-913.
34
35
36
37
38
39 13. Malik, R.; Khan, A. P.; Asangani, I. A.; Cieslik, M.; Prensner, J. R.; Wang, X.; Iyer, M.
40 K.; Jiang, X.; Borkin, D.; Escara-Wilke, J.; Stender, R.; Wu, Y. M.; Niknafs, Y. S.; Jing, X.;
41 Qiao, Y.; Palanisamy, N.; Kunju, L. P.; Krishnamurthy, P. M.; Yocum, A. K.; Mellacheruvu, D.;
42 Nesvizhskii, A. I.; Cao, X.; Dhanasekaran, S. M.; Feng, F. Y.; Grembecka, J.; Cierpicki, T.;
43 Chinnaiyan, A. M. Targeting the MLL complex in castration-resistant prostate cancer. *Nat. Med.*
44
45
46
47
48
49
50
51
52
53
54
55
56
57
58
59
60

- 1
2
3 14. Svoboda, L. K.; Bailey, N.; Van Noord, R. A.; Krook, M. A.; Harris, A.; Cramer, C.;
4
5 Jasman, B.; Patel, R. M.; Thomas, D.; Borkin, D.; Cierpicki, T.; Grembecka, J.; Lawlor, E. R.
6
7 Tumorigenicity of Ewing sarcoma is critically dependent on the trithorax proteins MLL1 and
8
9 menin. *Oncotarget* **2017**, *8* (1), 458-471.
10
11
12 15. Xu, B.; Li, S. H.; Zheng, R.; Gao, S. B.; Ding, L. H.; Yin, Z. Y.; Lin, X.; Feng, Z. J.;
13
14 Zhang, S.; Wang, X. M.; Jin, G. H. Menin promotes hepatocellular carcinogenesis and
15
16 epigenetically up-regulates Yap1 transcription. *Proc. Natl. Acad. Sci. U S A* **2013**, *110* (43),
17
18 17480-17485.
19
20
21 16. Kempinska, K.; Malik, B.; Borkin, D.; Klossowski, S.; Shukla, S.; Miao, H.; Wang, J.;
22
23 Cierpicki, T.; Grembecka, J. Pharmacologic inhibition of the menin-MLL interaction leads to
24
25 transcriptional repression of PEG10 and blocks hepatocellular carcinoma. *Mol. Cancer Ther.*
26
27 **2018**, *17* (1), 26-38.
28
29
30 17. Funato, K.; Major, T.; Lewis, P. W.; Allis, C. D.; Tabar, V. Use of human embryonic
31
32 stem cells to model pediatric gliomas with H3.3K27M histone mutation. *Science* **2014**, *346*
33
34 (6216), 1529-1533.
35
36
37 18. Fry, D. C. Protein-protein interactions as targets for small molecule drug discovery.
38
39 *Biopolymers* **2006**, *84* (6), 535-552.
40
41
42 19. Buchwald, P. Small-molecule protein-protein interaction inhibitors: therapeutic potential
43
44 in light of molecular size, chemical space, and ligand binding efficiency considerations. *IUBMB*
45
46 *Life* **2010**, *62* (10), 724-731.
47
48
49 20. Azzarito, V.; Long, K.; Murphy, N. S.; Wilson, A. J. Inhibition of alpha-helix-mediated
50
51 protein-protein interactions using designed molecules. *Nat. Chem.* **2013**, *5* (3), 161-173.
52
53
54
55
56
57
58
59
60

- 1
2
3 21. Wells, J. A.; McClendon, C. L. Reaching for high-hanging fruit in drug discovery at
4 protein-protein interfaces. *Nature* **2007**, *450* (7172), 1001-1009.
5
6
7 22. Arkin, M. R.; Whitty, A. The road less traveled: modulating signal transduction enzymes
8 by inhibiting their protein-protein interactions. *Curr. Opin. Chem. Biol.* **2009**, *13* (3), 284-290.
9
10
11 23. Smith, M. C.; Gestwicki, J. E. Features of protein-protein interactions that translate into
12 potent inhibitors: topology, surface area and affinity. *Expert Rev. Mol. Med.* **2012**, *14*, e16.
13
14
15 24. Cierpicki, T.; Grembecka, J. Targeting protein-protein interactions in hematologic
16 malignancies: still a challenge or a great opportunity for future therapies? *Immunol. Rev.* **2015**,
17 *263* (1), 279-301.
18
19
20 25. Bai, L.; Wang, S. Targeting apoptosis pathways for new cancer therapeutics. *Annu. Rev.*
21 *Med.* **2014**, *65*, 139-155.
22
23
24 26. Nero, T. L.; Morton, C. J.; Holien, J. K.; Wielens, J.; Parker, M. W. Oncogenic protein
25 interfaces: small molecules, big challenges. *Nat. Rev. Cancer* **2014**, *14* (4), 248-262.
26
27
28 27. Grembecka, J.; Belcher, A. M.; Hartley, T.; Cierpicki, T. Molecular basis of the mixed
29 lineage leukemia-menin interaction: implications for targeting mixed lineage leukemias. *J. Biol.*
30 *Chem.* **2010**, *285* (52), 40690-40698.
31
32
33 28. Murai, M. J.; Chruszcz, M.; Reddy, G.; Grembecka, J.; Cierpicki, T. Crystal structure of
34 menin reveals binding site for mixed lineage leukemia (MLL) protein. *J. Biol. Chem.* **2011**, *286*
35 (36), 31742-31748.
36
37
38 29. Huang, X. Fluorescence polarization competition assay: the range of resolvable inhibitor
39 potency is limited by the affinity of the fluorescent ligand. *J. Biomol. Screen.* **2003**, *8* (1), 34-38.
40
41
42
43
44
45
46
47
48
49
50
51
52
53
54
55
56
57

- 1
2
3 30. Brenner, E.; Baldwin, R. M.; Tamagnan, G. Asymmetric synthesis of (+)-(S,S)-
4 reboxetine via a new (S)-2-(hydroxymethyl)morpholine preparation. *Org. Lett.* **2005**, *7* (5), 937-
5 939.
6
7
8
9
10 31. Ghosh, M.; Seekamp, C. K.; Zhang, X.; Tarrant, J. G.; Lee, C.-W.; Kaiser, B.; Zablocki,
11 M. M.; Chenard, B. L.; Doller, D.; Yamaguchi, Y.; Wustrow, D. J.; Li, G. Aminopiperidines and
12 Related Compounds. U.S. Patent, WO2008016811A2, 2007.
13
14
15
16
17 32. Xu, S.; Aguilar, A.; Xu, T.; Zheng, K.; Huang, L.; Stuckey, J.; Chinnaswamy, K.;
18 Bernard, D.; Fernandez-Salas, E.; Liu, L.; Wang, M.; McEachern, D.; Przybranowski, S.; Foster,
19 C.; Wang, S. Design of the first-in-class, highly potent irreversible inhibitor targeting the menin-
20 MLL protein-protein interaction. *Angew. Chem. Int. Ed. Engl.* **2018**, *57* (6), 1601-1605.
21
22
23
24
25 33. Fairhead, M.; Howarth, M. Site-specific biotinylation of purified proteins using BirA.
26 *Methods Mol. Biol.* **2015**, *1266*, 171-184.
27
28
29
30 34. Otwinowski, Z.; Minor, W. [20] Processing of X-ray diffraction data collected in
31 oscillation mode. *Methods Enzymol.* **1997**, *276*, 307-326.
32
33
34
35 35. Murshudov, G. N.; Vagin, A. A.; Dodson, E. J. Refinement of macromolecular structures
36 by the maximum-likelihood method. *Acta Crystallogr. D Biol. Crystallogr.* **1997**, *53* (Pt 3), 240-
37 255.
38
39
40
41 36. Emsley, P.; Cowtan, K. Coot: model-building tools for molecular graphics. *Acta*
42 *Crystallogr. D Biol. Crystallogr.* **2004**, *60* (Pt 12 Pt 1), 2126-2132.
43
44
45 37. Collaborative Computational Project, N. The CCP4 suite: programs for protein
46 crystallography. *Acta Crystallogr. D Biol. Crystallogr.* **1994**, *50* (Pt 5), 760-763.
47
48
49
50 38. Adams, P. D.; Afonine, P. V.; Bunkoczi, G.; Chen, V. B.; Davis, I. W.; Echols, N.;
51 Headd, J. J.; Hung, L. W.; Kapral, G. J.; Grosse-Kunstleve, R. W.; McCoy, A. J.; Moriarty, N.
52
53
54
55
56
57
58
59
60

- 1
2
3 W.; Oeffner, R.; Read, R. J.; Richardson, D. C.; Richardson, J. S.; Terwilliger, T. C.; Zwart, P.
4
5 H. PHENIX: a comprehensive Python-based system for macromolecular structure solution. *Acta*
6
7 *Crystallogr. D Biol. Crystallogr.* **2010**, *66* (Pt 2), 213-221.
8
9
10 39. Davis, I. W.; Leaver-Fay, A.; Chen, V. B.; Block, J. N.; Kapral, G. J.; Wang, X.; Murray,
11
12 L. W.; Arendall, W. B., 3rd; Snoeyink, J.; Richardson, J. S.; Richardson, D. C. MolProbity: all-
13
14 atom contacts and structure validation for proteins and nucleic acids. *Nucleic Acids Res.* **2007**, *35*
15
16 (Web Server issue), W375-W383.
17
18
19 40. Yang, H.; Guranovic, V.; Dutta, S.; Feng, Z.; Berman, H. M.; Westbrook, J. D.
20
21 Automated and accurate deposition of structures solved by X-ray diffraction to the Protein Data
22
23 Bank. *Acta Crystallogr. D Biol. Crystallogr.* **2004**, *60* (Pt 10), 1833-1839.
24
25
26 41. Muntean, A. G.; Tan, J.; Sitwala, K.; Huang, Y.; Bronstein, J.; Connelly, J. A.; Basrur,
27
28 V.; Elenitoba-Johnson, K. S.; Hess, J. L. The PAF complex synergizes with MLL fusion proteins
29
30 at HOX loci to promote leukemogenesis. *Cancer Cell* **2010**, *17* (6), 609-621.
31
32
33 42. Krueger, A. C.; Madigan, D. L.; Jiang, W. W.; Kati, W. M.; Liu, D.; Liu, Y.; Maring, C.
34
35 J.; Masse, S.; McDaniel, K. F.; Middleton, T.; Mo, H.; Molla, A.; Montgomery, D.; Pratt, J. K.;
36
37 Rockway, T. W.; Zhang, R.; Kempf, D. J. Inhibitors of HCV NS5B polymerase: synthesis and
38
39 structure-activity relationships of N-alkyl-4-hydroxyquinolon-3-yl-benzothiadiazine sulfamides.
40
41
42 *Bioorg. Med. Chem. Lett.* **2006**, *16* (13), 3367-3370.
43
44
45
46
47
48
49
50
51
52
53
54
55
56
57
58
59
60

Figure legends

Figure 1. Structures and binding mode of the previous generation of menin-MLL inhibitors. **a)** Chemical structures of the thienopyrimidine menin-MLL inhibitors **MI-463**, **MI-503** and **MI-538** together with the inhibitory activity of these compounds measured in the fluorescence polarization (FP) competition assays with menin and the fluorescein labeled MLL₄₋₁₅ or MLL₄₋₄₃ peptides. **b)** Crystal structure of menin in complex with **MI-503** (4X5Y in PDB). Protein is shown in ribbon representation and key menin residues involved in interactions with **MI-503** are shown as sticks. **MI-503** is shown in stick representation with colors corresponding to the atom type (green: carbons, dark blue: nitrogens, yellow: sulfur, light blue: fluorine). Dashed lines represent hydrogen bonds between **MI-503** and menin.

Figure 2. Structure-based optimization results in potent menin-MLL inhibitors. **a)** Crystal structure of the menin-compound **13** complex (PDB code 6BXH). Residues on menin involved in the interactions with the piperazine ring and the terminal amide of **13** are shown in stick representation. Hydrogen bond with Arg330 is marked. **b)** Crystal structure of the menin-compound **28** complex (PDB code 6BXY). Residues on menin involved in the interactions with the morpholinone ring in **28** are shown in stick representation. Hydrogen bond with Glu366 is marked. **c)** Superposition of the crystal structures of menin in complex with **MI-503**, **28** and MLL peptide encompassing MBM1 and MBM2 motifs (3U88 in PDB). **d)** Comparison of the binding mode of **28** (left) and **29** (right, PDB code 6BY8) to menin.

Figure 3. Inhibition of the menin-MLL interaction and cellular activity of compound 28. **a)** Titration curves from the FP competition assay for inhibition of the menin-MLL₄₋₄₃ by **28** and **29**. Data represent mean values of duplicate samples \pm SD. **b-d)** Titration curves from the MTT cell viability assay performed for **28** or **29** after 7 days of treatment of: MLL-AF9 or

1
2
3 Hoxa9/Meis1 (HM-2) transformed murine bone marrow cells treated with **28** (**b**), human MLL
4 leukemia cell lines (MV4;11 and MOLM-13) and control cell lines (K562 and U937 without
5 MLL translocation) treated with **28**, (**c**); human MLL leukemia cell lines treated with **29** (**d**). Cell
6 growth inhibition (GI_{50}) values are provided. Data represent mean values of quadruplicates \pm SD.
7
8 The experiments were performed 2 times. Values are normalized with respect to DMSO treated
9 samples. **e**) qRT-PCR performed in MV4;11 cells after 6 days of treatment with **28**. Expression
10 of *HOXA9*, *MEIS1*, *DLX2* and *ITGAM* was normalized to 18S and referenced to DMSO-treated
11 cells, mean \pm SD, n = 2.
12
13
14
15
16
17
18
19
20
21

22 **Figure 4. Compound 28 strongly inhibits leukemia progression in mice. a, b)**
23 Bioluminescence level in MV4;11 leukemia mice measured at days 0, 7, 14 and 21 after
24 initiating treatment with vehicle or **28**. n = 8 mice per group. **b)** Representative images of
25 MV4;11 mice treated with vehicle or **28** at day 21 of treatment. **c)** Spleen weight and pictures of
26 MV4;11 mice after 6 days of treatment with vehicle or **28** (n = 3 mice / group). **d)** Level of
27 hCD45+ cells in MV4;11 mice after 6 days of treatment with vehicle or **28** measured by flow
28 cytometry (n = 3 mice / group). **e)** Expression of *HOXA9*, *MEIS1* and *ITGAM* in the bone
29 marrow (BM) and spleen samples of the MV4;11 leukemia mice after 6 days of treatment with
30 **28**. Expression was normalized to GAPDH and referenced to vehicle treated mice, mean \pm SD, n
31 = 3.
32
33
34
35
36
37
38
39
40
41
42
43
44
45
46
47
48
49
50
51
52
53
54
55
56
57
58
59
60

Figure 1

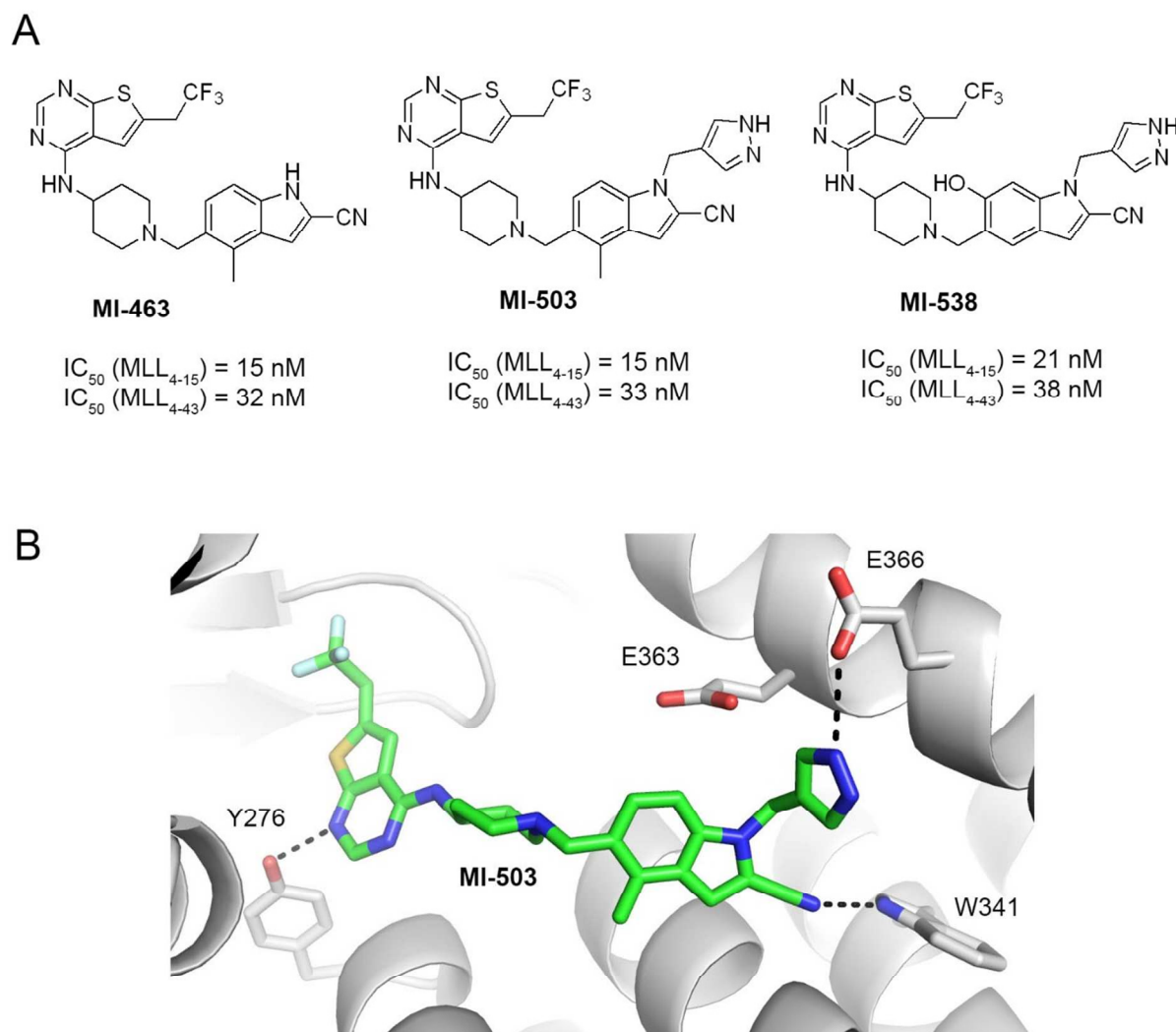


Figure 2

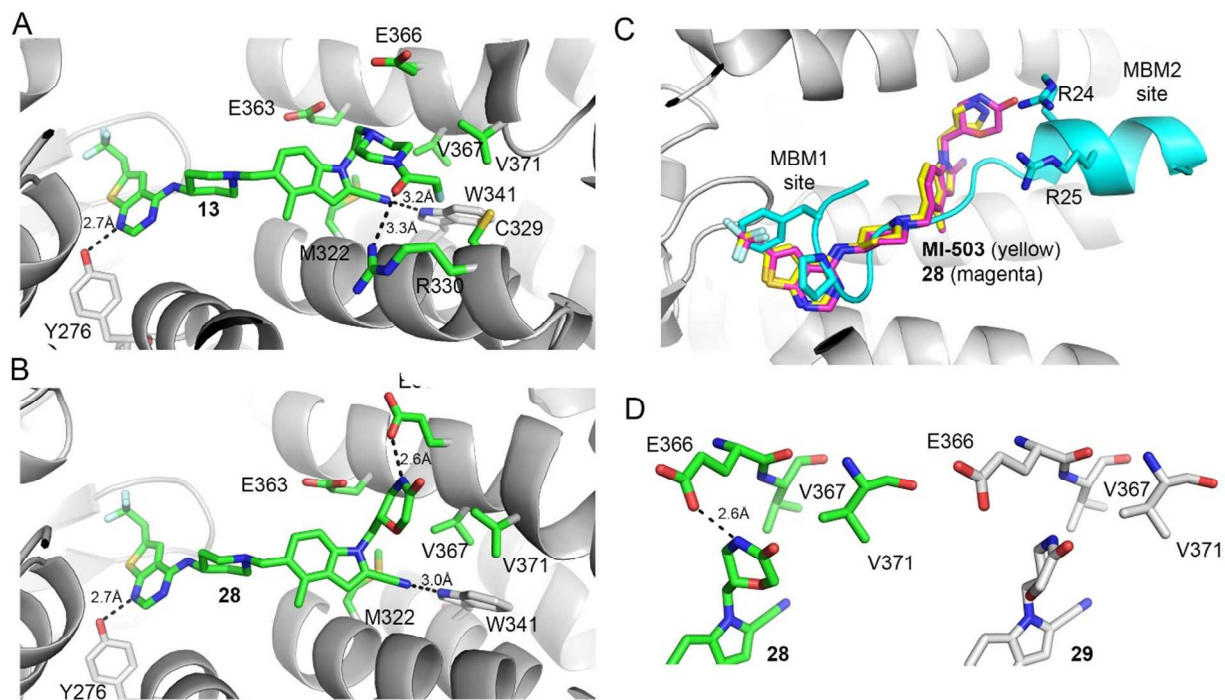


Figure 3

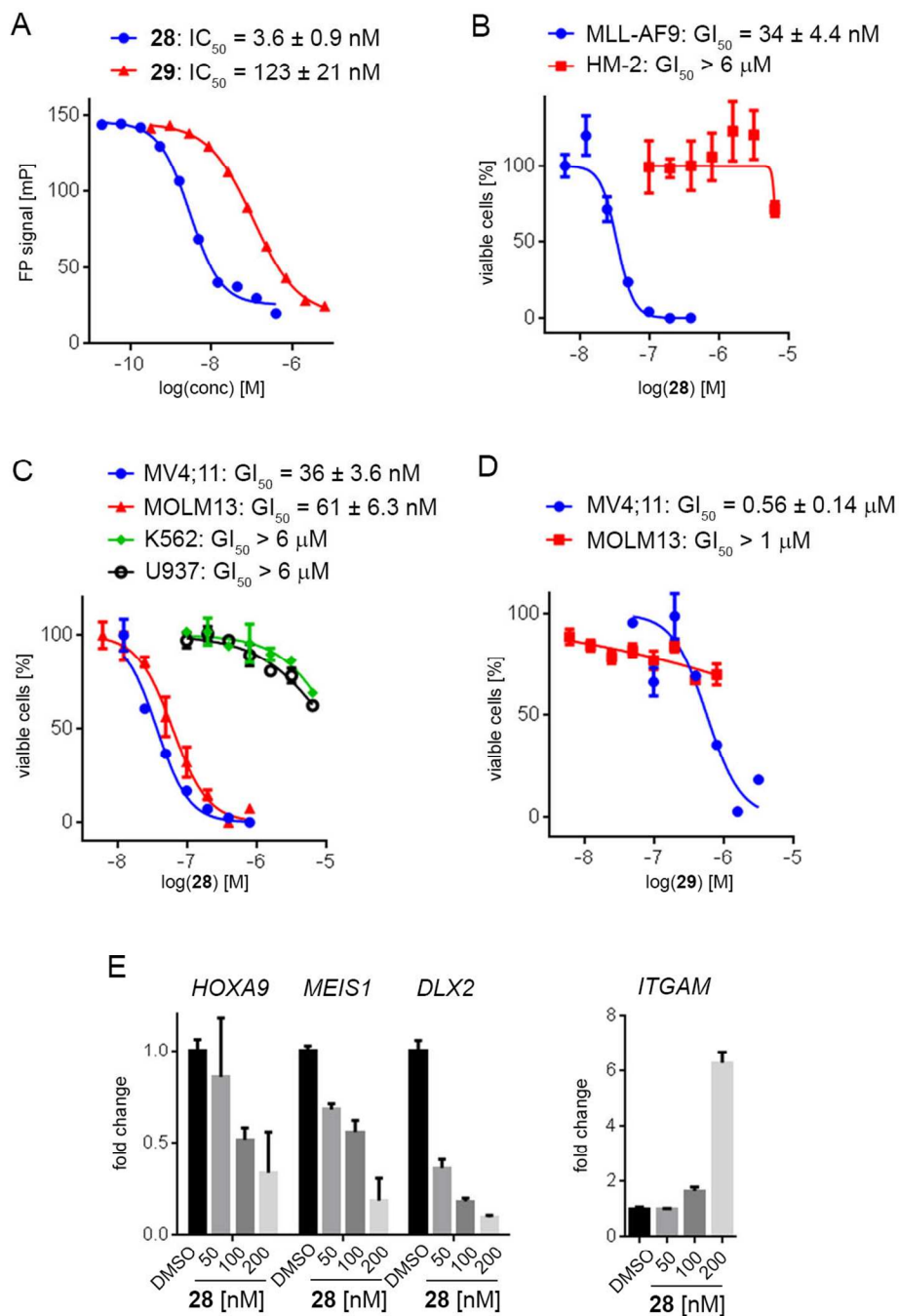
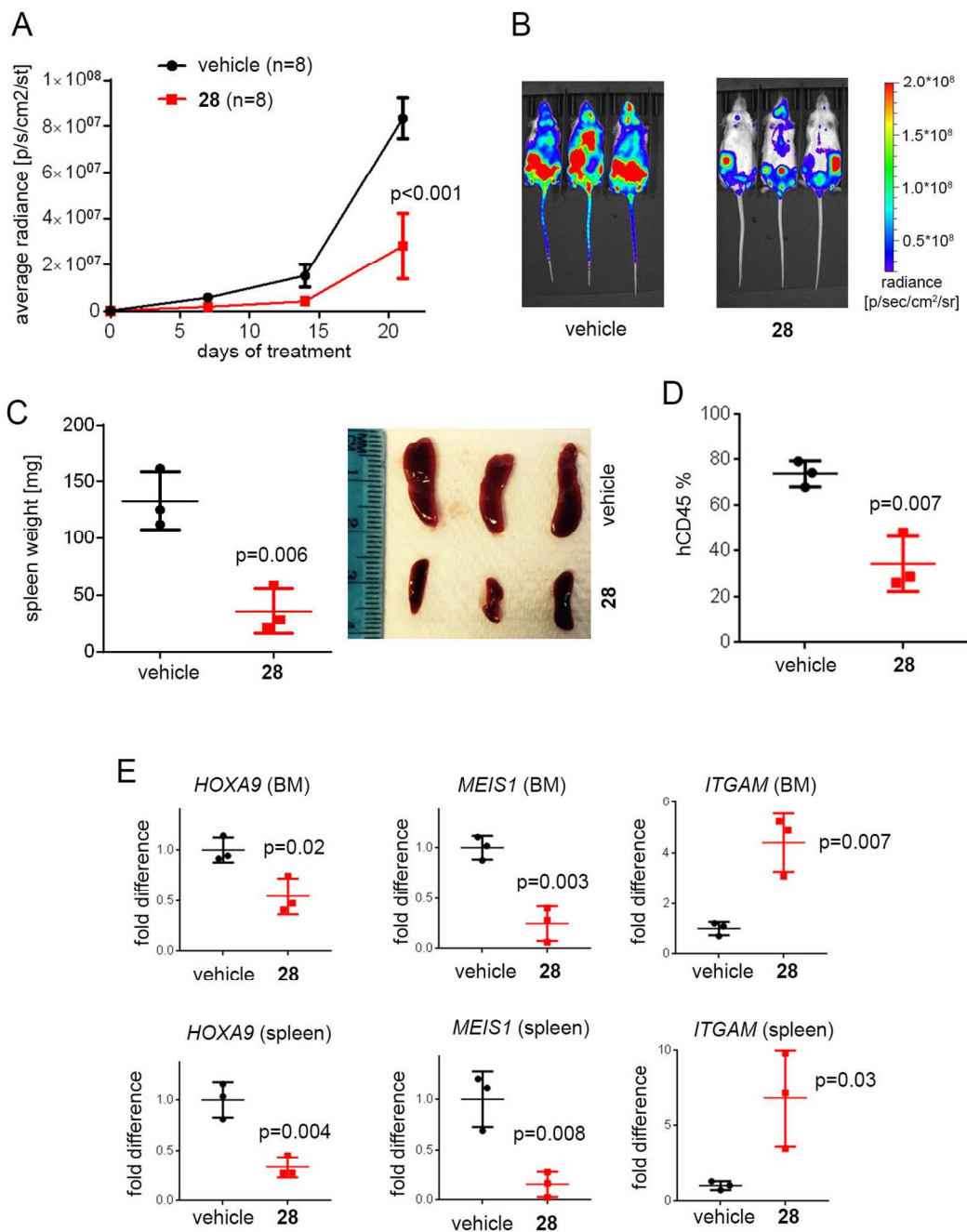
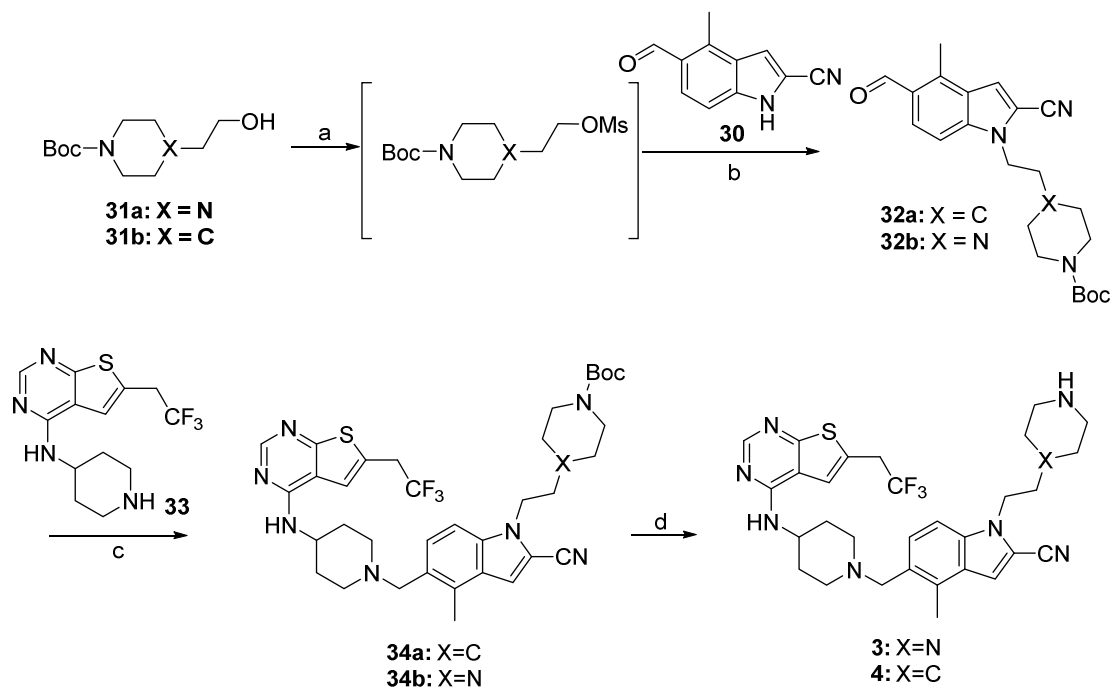
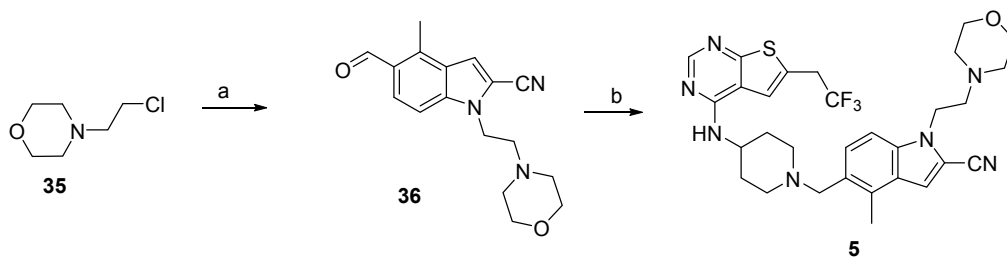


Figure 4

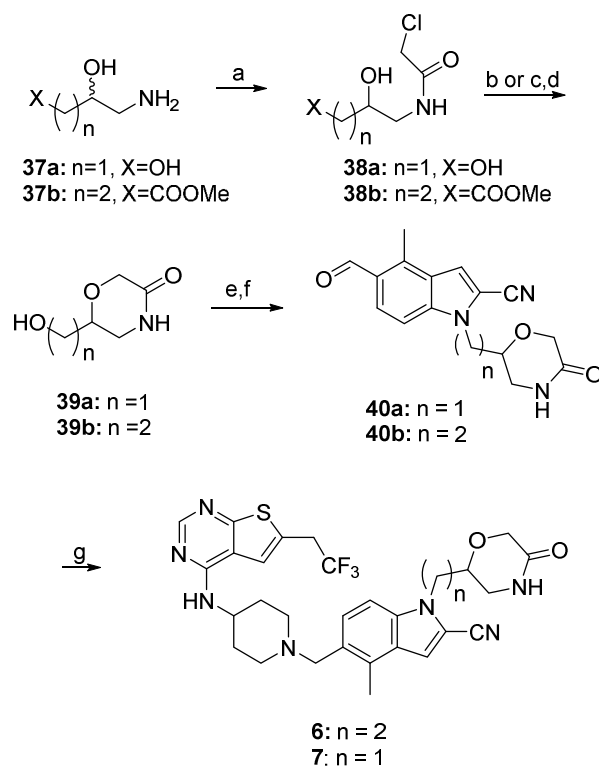


Scheme 1. Synthesis of compounds **3** and **4**^a

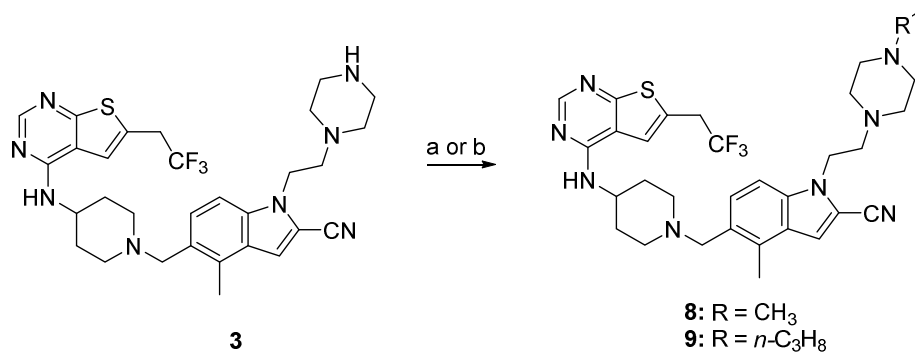
^a Reagents and conditions: a) MsCl, TEA, DCM -67°C- rt; b) **30**, Cs₂CO₃, DMF, 90-110°C; c) **33**, Na(AcO)₃BH; TEA, rt; d) SnCl₄, tartaric acid.

Scheme 2: Synthesis of compound 5.^a

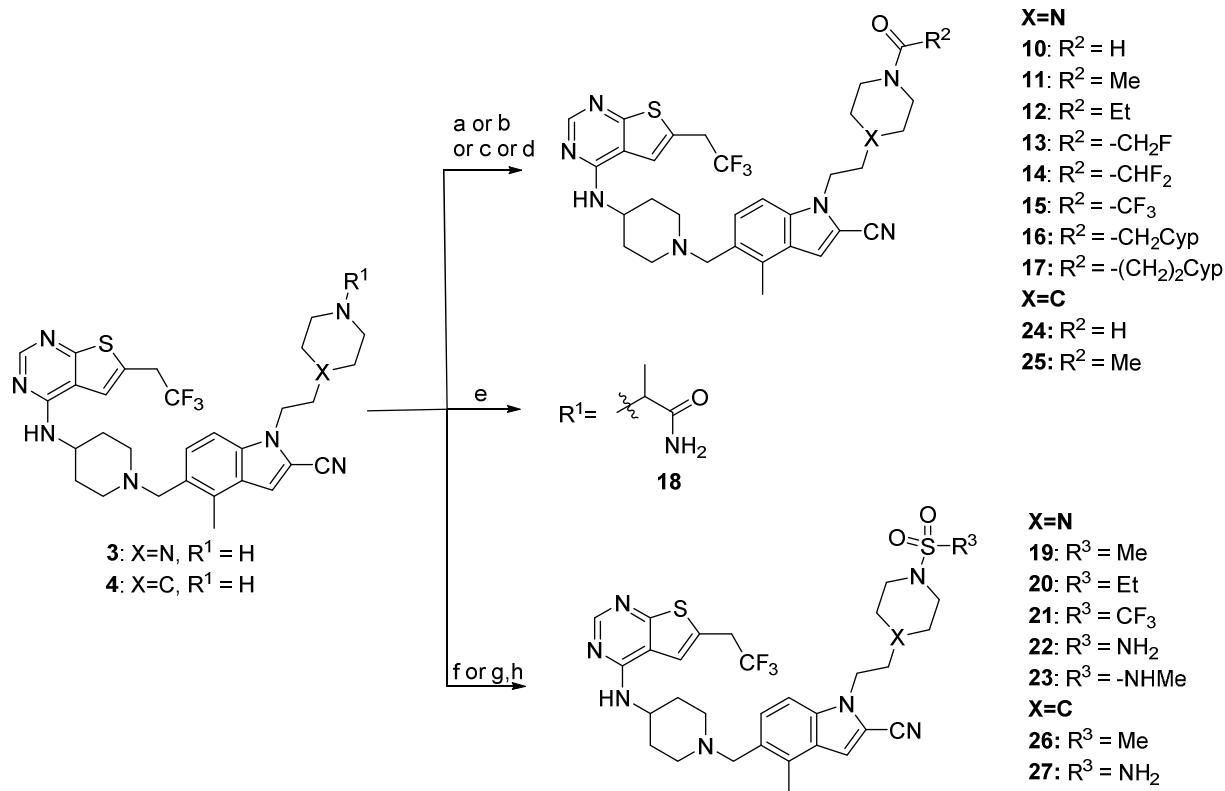
^a Reagents and conditions: a) **30**, Cs₂CO₃, TBAI, DMF, 90°C; b) **33**, Na(AcO)₃BH; TEA, rt.

Scheme 3: Synthesis of compounds **6** and **7**^a

^a Reagents and conditions: a) chloroacetic acid chloride, MeOH, AcCN, TEA, 0°C; b) *t*-BuOK, amyl alcohol, rt (for **38a**); c) LiBH₄, THF, 0°C and d) *t*-BuOK, amyl alcohol, 0°C (for **38b**); e) MsCl, TEA, DCM, -67°C- rt; f) **30**, Cs₂CO₃, DMA, 105°C; g) **33**, Na(AcO)₃BH; AcOH, 50°C.

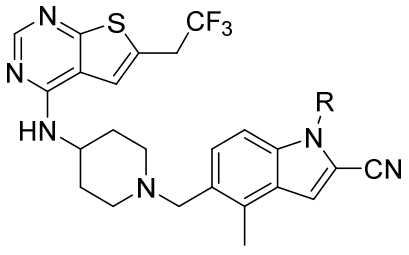
Scheme 4: Synthesis of compounds **8** and **9**^a

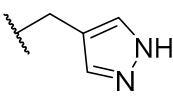
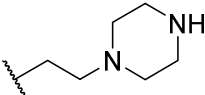
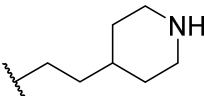
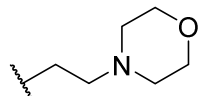
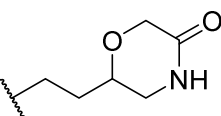
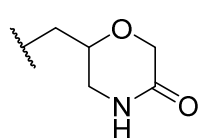
^a Reagents and conditions: a) formaline, Na(AcO)₃BH, AcCN, rt (for **8**); b) *n*-propanal, Na(AcO)₃BH; TEA, DCM, rt (for **9**).

Scheme 5: Synthesis of compounds 10-27^a

^a Reagents and conditions: a) HCOOMe, reflux (for **10,24**); b) R²COCl, DIPEA, DCM or AcCN, rt (for **11,12,17, 25**); c) R²COOH, TBTU, THF (for **13,14,16**); d) (CF₃CO)₂O, DCM, 0°C-rt (for **15**); e) *rac*-BrCH(CH₃)CONH₂, DMF (for **18**); f) R¹SO₂Cl; DIPEA, DCM, rt (for **19,20,21,23,26**); g) CbzNHSO₂Cl, DIPEA, DCM and h) Pd/C, MeOH, ammonium formate (for **22,27**).

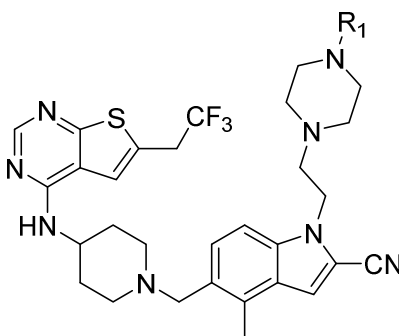
Table 1. Structure-Activity Relationship (SAR) and properties of MI-463 derivatives with various rings introduced at indole nitrogen.



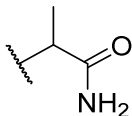
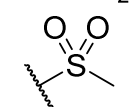
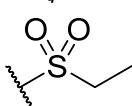
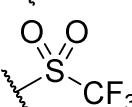
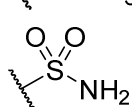
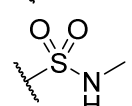
Compound	R	IC ₅₀ MLL ₄₋₄₃ (nM) ^a	GI ₅₀ (μM) ^b MLL-AF9	T _{1/2} (min) ^c	cLogP ^d
1 (MI-463)	H	32 ± 9.9	0.23	14	4.7
2 (MI-503)		33 ± 8.5	0.22	21	4.4
3		15 ± 4.9	0.52	>60	4.3
4		14 ± 1.4	0.81	>60	5.5
5		22 ± 5.7	0.24	<3	4.7
6 (RS)		28 ± 4.9	0.15	31	4.1
7 (RS) (MI-568)		7.5 ± 2.1	0.05	>60	3.7

^a IC₅₀ values were measured by fluorescence polarization assay using fluorescein labeled MLL₄₋₄₃, average values from 2-3 independent measurements ± SD are provided. ^b Growth inhibition (GI₅₀ values) measured in the MTT cell viability assay after 7 days of treatment of murine bone marrow cells transformed with MLL-AF9. ^c Half-life of compounds in mouse liver microsomes. ^d Calculated with ChemBioDraw Ultra 14.0.

Table 2. SAR and properties of N-substituted analogues of compound 3.

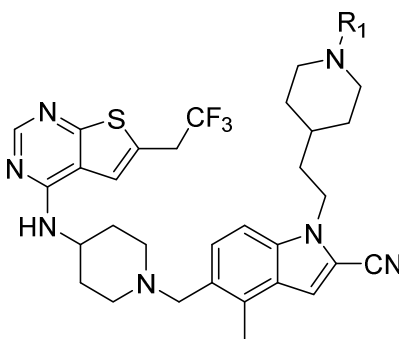


Compound	R ₁	IC ₅₀ MLL ₄₋₄₃ (nM) ^a	GI ₅₀ (μM) ^b MLL-AF9	T _{1/2} (min) ^c	cLogP ^d
3	H	15 ± 4.9	0.40	>60	4.3
8		13 ± 0.7	0.23	9.2	3.8
9		39 ± 2.1	1.0	12	4.9
10		13 ± 4.2	0.15	21	4.1
11		18 ± 3.5	0.15	13	4.2
12		83 ± 2.8	0.25	13	4.8
13 (MI-853)		10 ± 0.7	0.075	5.7	4.5
14		44 ± 17	0.18	4.9	4.8
15		75 ± 22	0.23	14	5.4
16		57 ± 8.5	1.2	8.6	6.4
17		42 ± 2.8	0.75	10	6.9

18 (<i>RS</i>)		21 ± 4.2	0.25	11	3.2
19		13 ± 2.8	0.15	26	4.7
20		55 ± 15	0.25	19	5.2
21		71 ± 7.1	0.45	15	5.8
22		26 ± 2.1	0.22	53	4.7
23		32 ± 1.4	0.15	24	4.4

^a IC₅₀ values were measured by fluorescence polarization assay using fluorescein labeled MLL₄₋₄₃, average values from 2-3 independent measurements ± SD are provided. ^b Growth inhibition (GI₅₀ values) measured in the MTT cell viability assay after 7 days of treatment of murine bone marrow cells transformed with MLL-AF9. ^c Half-life of compounds in mouse liver microsomes. ^d Calculated with ChemBioDraw Ultra 14.0.

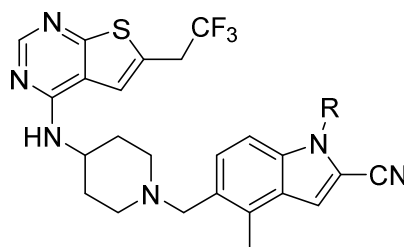
Table 3. SAR and properties of N-substituted analogues of compound 4.



Compound	R	IC ₅₀ MLL ₄₋₄₃ (nM) ^a	GI ₅₀ (μM) ^b MLL-AF9	T _{1/2} (min) ^c	cLogP ^d
4	H	14 ± 1.4	0.81	>60	5.5
24		63 ± 2.1	0.57	25	4.6
25		130 ± 32	0.97	26	4.6
26		40 ± 9.2	0.25	>60	5.2
27		38 ± 10	0.35	>60	5.6

^a IC₅₀ values were measured by fluorescence polarization assay using fluorescein labeled MLL₄₋₄₃, average values from 2-3 independent measurements ± SD are provided. ^b Growth inhibition (GI₅₀ values) measured in the MTT cell viability assay after 7 days of treatment of murine bone marrow cells transformed with MLL-AF9. ^c Half-life of compounds in mouse liver microsomes. ^d Calculated with ChemBioDraw Ultra 14.0.

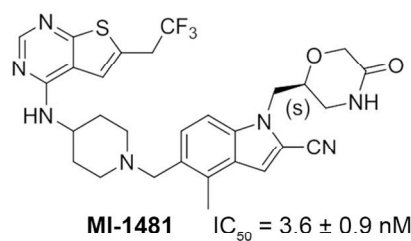
Table 4. SAR and properties of enantiomers of compound 7.



Compound	R	IC ₅₀ MLL ⁴⁻⁴³ (nM) ^a	GI ₅₀ (μM) ^b MLL-AF9	SI	T _{1/2} (min) ^c	cLogP ^d
7 (RS) (MI-568)		7.5 ± 2.1	0.05	180	>60	3.7
28 (S) (MI-1481)		3.6 ± 0.9	0.034	>180	59	3.7
29 (R) (MI-1482)		122 ± 22	0.7	ND	>60	3.7

^a IC₅₀ values were measured by fluorescence polarization assay using fluorescein labeled MLL⁴⁻⁴³, average values from 2-3 independent measurements ± SD are provided. ^b Growth inhibition (GI₅₀ values) measured in the MTT cell viability assay after 7 days of treatment of murine bone marrow cells transformed with MLL-AF9. ^c Half-life of compounds in mouse liver microsomes. ^d Calculated with ChemBioDraw Ultra 14.0. SI, selectivity index calculated as a ratio of GI₅₀ values measured in HM-2 cells (control cell line) and MLL-AF9 transformed murine bone marrow cells. ND – not determined.

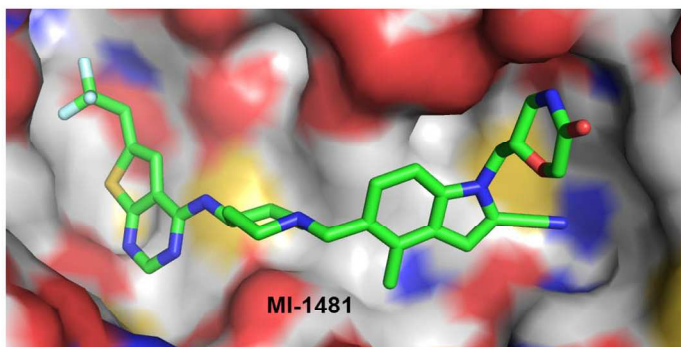
Table of Contents Graphic

**MLL fusion cell lines**

MV4;11: $GI_{50} = 36 \pm 3.6$ nM
MOLM13: $GI_{50} = 61 \pm 6.3$ nM

**non-MLL fusion
cell lines**

K562: $GI_{50} > 6$ μ M
U937: $GI_{50} > 6$ μ M

**MLL leukemia model**